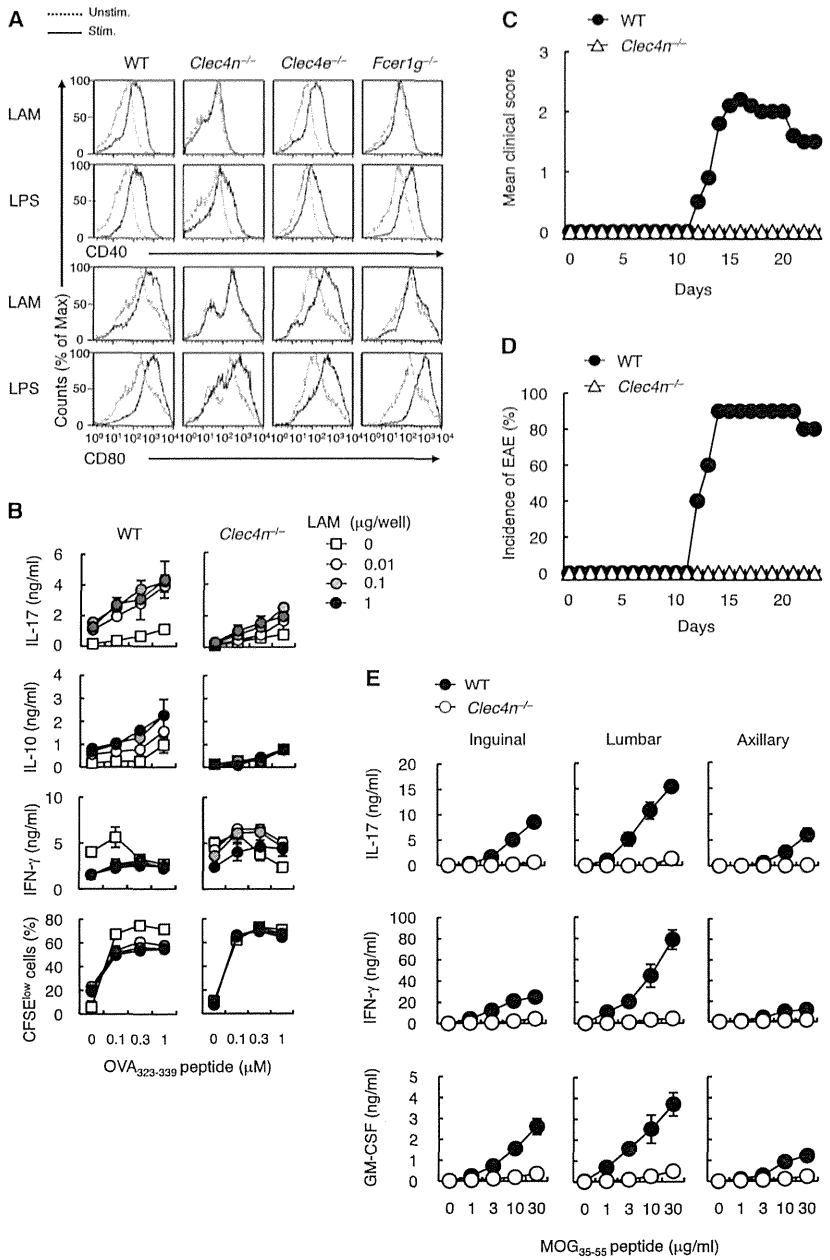

Figure 6. LAM Induces Acquired Immune Responses through Dectin-2

(A) BMDCs obtained from WT, *Clec4n*$^{-/-}$, *Clec4e*$^{-/-}$, or *Fcer1g*$^{-/-}$ mice were left untreated or stimulated with plate-coated LAM or LPS for 48 hr. The surface expressions of CD40 and CD80 were analyzed using flow cytometry.

(B) BMDCs were pulsed with $OVA_{323-339}$ peptides and cocultured with CFSE-labeled $CD4^+$ OT-II T cells for 3 days in the presence or absence of plate-coated LAM. Cytokine concentrations were determined using ELISA. Cell proliferation was analyzed using flow cytometry for dilution of CFSE within the $CD4^+$ population. The data are presented as the means ± SD of triplicate and are representative of three separate experiments.

(C and D) WT (n = 10) and *Clec4n*$^{-/-}$ (n = 10) mice were immunized with MOG_{35-55} peptide in IFA containing LAM (500 μg) as described in Figure 1A. Mean clinical score (C) and disease incidence (D) at the indicated times were plotted.

(E) Lymph nodes were collected at 23 days after immunization for EAE and stimulated with MOG_{35-55} peptide for 4 days. Cytokine concentrations were determined using ELISA. The data are presented as the means ± SD.

See also Figure S5.

functions to promote IL-17 production in a Dectin-2-dependent manner.

Man-LAM Promotes Antigen-Specific Human T Cell Responses through Human Dectin-2

We then assessed whether Man-LAM influences human T cell responses as observed in murine T cells. Importantly, Man-LAM activated reporter cells expressing hDectin-2, and this activity was blocked in the presence of anti-hDectin-2 mAb (Figure S5B). The Man-LAM-induced cytokine production in human monocytes and monocyte-derived DCs was also significantly suppressed by anti-hDectin-2 mAb (Figures S5C and S5D). Peripheral blood mononuclear cells (PBMCs) from tuberculosis patients were stimulated with C10 peptide (VVRFQEAANKQKQEL) of CFP-10 (10 kDa culture filtrate antigen) from *M. tuberculosis*. Antigen peptides alone induced a substantial amount of IFN-γ production in PBMCs, whereas it was augmented upon Man-LAM stimulation in combination with antigen peptides. Man-LAM-induced augmentation of IFN-γ production was markedly compromised in the presence of anti-hDectin-2 mAb (Figure S5E). The Dectin-2-dependent enhancement of IFN-γ production was also observed in three other individuals (Figure S5F). These results indicate that Man-LAM-hDectin-2 interaction promotes the mycobacterial antigen-specific responses of T cells from tuberculosis patients, presumably through the activation of myeloid cells in PBMCs.

Man-LAM induced weak T cell proliferation in T cell-DC coculture even in the absence of antigen, which also required Dectin-2 on DCs (Figure 6B). This "antigen-independent proliferation" might be conferred by a large amount of IL-2 secretion through Dectin-2 on DCs (Figure 4C), because the addition of anti-IL-2 neutralizing mAb ablated this response (Figure S5A).

In contrast to the enhancement of IL-17 production, Man-LAM treatment had essentially no effect on the antigen-dependent IFN-γ production (Figure 6B). IL-4 was not detected at any time point in this experiment (data not shown). Collectively, these in vitro results suggest that Man-LAM stimulation enhances APC

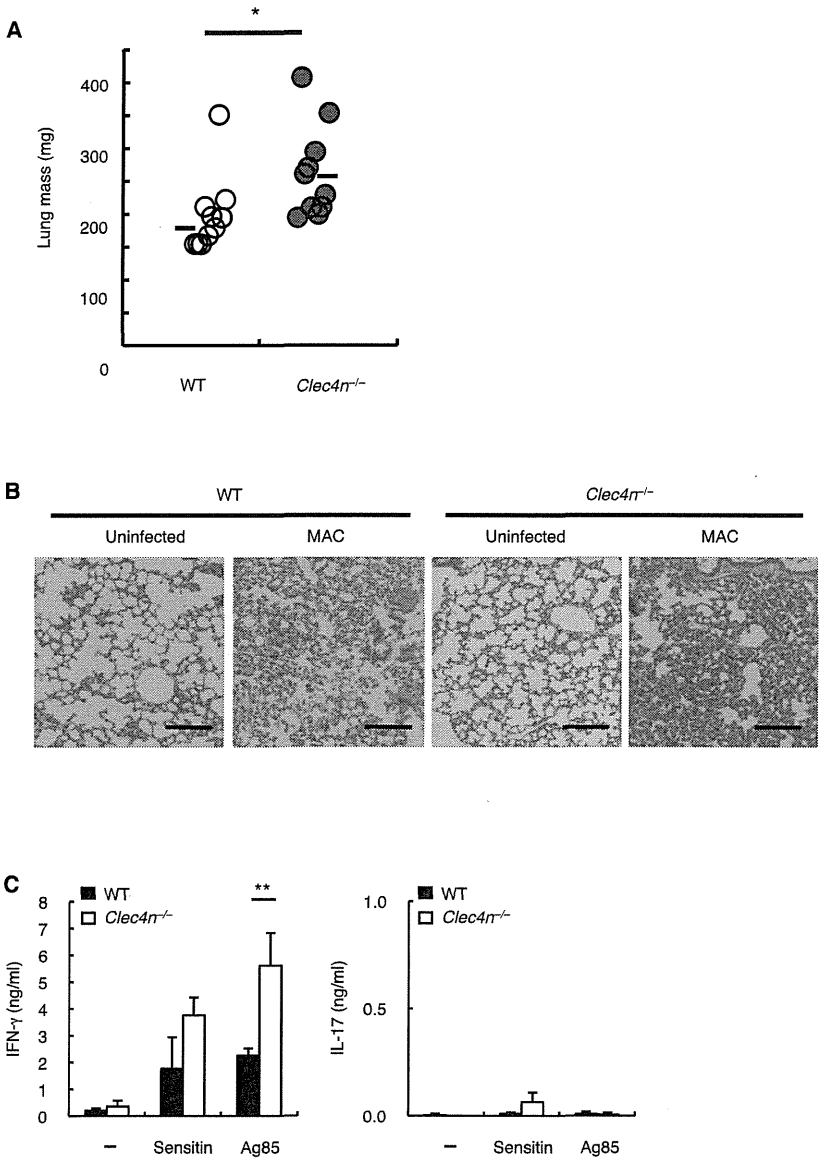

Figure 7. Immune Responses against Mycobacterial Infection in *Clec4n*$^{-/-}$ Mice

(A) Higher lung weights in *Clec4n*$^{-/-}$ mice. Lungs were isolated 23 days after infection of MAC. WT (n = 10) and *Clec4n*$^{-/-}$ (n = 10) mice were used.

(B) Histological analysis of the lung from uninfected- or MAC-infected WT or *Clec4n*$^{-/-}$ mice by HE staining. Scale bars represent 0.1 mm.

(C) Cytokine production in splenocytes after restimulation with sensitin or MACAg85 for 4 days. Splenocytes were obtained 23 days after infection of MAC and pooled from ten mice in each group. The data are presented as mean ± SD.

See also Figure S6.

Induction of EAE through Man-LAM Immunization via Dectin-2-FcRγ Axis

We next performed a murine model of T helper 17 (Th17) cell-mediated autoimmune disease, EAE, since Dectin-2 activation by Man-LAM induced IL-17 production in vitro (Figure 6B). Strikingly, *Clec4n*$^{-/-}$ mice were completely resistant to Man-LAM-induced EAE (Figures 6C and 6D), indicating that other Man-LAM receptors cannot compensate for the loss of Dectin-2 in vivo. Furthermore, ex vivo recall responses, as assessed by the production of IL-17, IFN-γ, and GM-CSF, of the lymph node cells collected from inguinal, lumbar, and axillary lymph nodes were completely abrogated in *Clec4n*$^{-/-}$ mice (Figure 6E). This indicates that Man-LAM cannot efficiently prime T cells in Dectin-2-deficient environment. Taken together, Dectin-2 is a receptor essential for the adjuvanticity of Man-LAM in vivo.

Role of Dectin-2 in Mycobacterial Infection

Finally, we examined the role of Dectin-2 in mycobacterial infection in vivo. WT and *Clec4n*$^{-/-}$ mice were infected intranasally with *M. avium* complex (MAC). Although the bacterial burden in the lungs was not significantly altered at 3 weeks after infection, the average number of colony forming units (CFU) per lungs was larger in *Clec4n*$^{-/-}$ mice than in WT mice (WT, 6.54 ± 6.47; *Clec4n*$^{-/-}$, 13.1 ± 8.32 [× 10^2]). We therefore characterized the lung pathology of infected mice. Lung swelling as assessed from lung mass was significantly greater in *Clec4n*$^{-/-}$ mice (Figure 7A). In addition, *Clec4n*$^{-/-}$ mice presented with increased histopathology in the lungs after infection (Figure 7B). Chemokine concentrations were elevated in the lungs of *Clec4n*$^{-/-}$ mice compared with WT mice 3 weeks after infection (Figure S6). These chemokines seemed to be induced by bacteria residing in the lungs, because the chemokine concentration in each individual mouse was correlated with the bacterial burden in the lungs (data not shown). The production of cytokines, such as TNF, IL-6, and IL-10, were not elevated in the lungs of WT and *Clec4n*$^{-/-}$ mice at day 23 after infection (data not shown). We also examined antigen-specific T cell responses in the infected mice. Splenic T cells from *Clec4n*$^{-/-}$ mice produced a significantly larger amount of IFN-γ upon recall stimulation by mycobacterial antigens, whereas IL-17 production was not altered (Figure 7C). Thus, Dectin-2 deficiency resulted in augmented lung pathology and acquired immunity presumably due to the inefficient elimination of mycobacteria. Collectively, these results suggest that Dectin-2 is involved in host defense against mycobacteria.

DISCUSSION

In this manuscript, we have demonstrated that Dectin-2 is a direct and functional receptor for mycobacterial Man-LAM.

Mincle, MCL, and Dectin-2 are located in the same gene cluster, and we found that all these CLRs recognize mycobacteria (Ishikawa et al., 2009; Miyake et al., 2013). The acquisition of different CLRs recognizing distinct mycobacterial components during evolution would enable the host to exert stable immune responses against this life-threatening bacteria.

Dectin-2 has been reported to recognize high-mannose structures of fungi (McGreal et al., 2006), such as α-1,2-mannan derived from *Candida albicans* (Robinson et al., 2009; Saijo et al., 2010) and mannoprotein from *Malassezia* fungus (Ishikawa et al., 2013). Glycan array analysis confirms that Dectin-2 preferentially binds to high-mannose structures, similar to DC-SIGN, SIGNR1, SIGNR3, and MMR (McGreal et al., 2006), all of which possess the mannose-binding EPN sequence within their carbohydrate recognition domains (CRDs) (Drickamer, 1992). Man-LAM possesses polysaccharide chains that terminates in a α-1,2-mannose cap (Mishra et al., 2011). It is highly likely that the α-1,2-linked mannose residues of Man-LAM are the direct determinant recognized by Dectin-2.

Man-LAM is densely distributed in the envelopes of mycobacteria with the specific configuration, and thereby their polar mannose caps are exposed on the bacterial surface with oligomeric valency. The multivalent α-1,2-mannose residue is not inconsistent with the characteristics of PAMPs recognized by Dectin-2 (Ishikawa et al., 2013; Saijo et al., 2010). To replicate this configuration in vitro, Man-LAM was used as plate-coated form to evaluate Dectin-2-mediated responses in this study. Previous studies show that soluble Man-LAM alone does not induce cytokine production in myeloid cells (Geijtenbeek et al., 2003; Gringhuis et al., 2009; Nigou et al., 2001) and we confirmed this with BMDCs (data not shown). These different outcomes depending on the stimuli might be attributed to the difference in the receptor engagement caused by the nature of the ligand—monovalent (soluble) versus multivalent (immobilized). It has been demonstrated that soluble Man-LAM influences myeloid cell function in the presence of other stimuli such as TLR ligands (Geijtenbeek et al., 2003; Gringhuis et al., 2007; Nigou et al., 2001). One possible explanation for these findings is that TLR-bound lipoprotein might provide a scaffold for soluble Man-LAM through hydrophilic interaction in aqueous media, which leads to ligand multimerization sufficient for the engagement of Dectin-2. Consistent with these ideas, multimerized Man-LAM in oil emulsion exhibited potent adjuvant activity in vivo. Collectively, Dectin-2 might discriminate multivalent PAMPs presented on "real" pathogens, presumably to prevent false recognition of their targets.

The α-1,2-linked mannose residues are also present in phosphatidyl-*myo*-inositol mannosides (PIMs). Because PIMs have been shown to be potentially associated with MMR and DC-SIGN (Torrelles et al., 2006), Dectin-2 might recognize PIMs. However, *M. abscessus*, which lacks Man-LAM but possesses PIMs, did not activate reporter cells expressing Dectin-2, implying that PIMs might not be a potent ligand for Dectin-2. Alternatively, Dectin-2 may not be able to access "short" PIMs within "tall" cell wall components, such as long-chain mycolic acids, glycolipids, lipoglycans, and polysaccharides (Mishra et al., 2011; Torrelles et al., 2006).

SIGNR1, SIGNR3, and MMR have been reported as murine receptors for Man-LAM (Koppel et al., 2004; Schlesinger et al., 1994; Tanne et al., 2009). Peritoneal macrophages from *Cd209b*$^{-/-}$ mice produce less, but detectable, IL-10 in response to Man-LAM (Wieland et al., 2007). However, gene ablation of SIGNR1 and anti-MMR blocking mAb did not influence the LAM-induced cytokine production in BMDCs. SIGNR3 is not expressed on BMDCs and forced expression of SIGNR3 did not rescue cytokine production in *Clec4n*$^{-/-}$ BMDCs. Thus, the characteristic cytokine production induced by Man-LAM seems to be determined by intrinsic signaling via Dectin-2 in DCs. Although Man-LAM-induced in vivo responses were also completely abolished in *Clec4n*$^{-/-}$ mice, it is possible that SIGNR3 plays a role in Man-LAM responses in particular cells, such as dermal DCs, that express SIGNR3 (Nagaoka et al., 2010). Alternatively, these Man-LAM-binding molecules might promote the binding of myeloid cells to Man-LAM-bearing bacteria (Tanne et al., 2009), thereby leading to the efficient phagocytosis of mycobacteria.

Our data demonstrate that Man-LAM is a sufficient component to trigger IL-10 production. However, we cannot exclude the possibility that Man-LAM is not necessarily required for IL-10 production induced by whole mycobacteria, although NTM strain *M. abscessus* lacking Man-LAM did not induce IL-10 production. The results from mutant *M. bovis* BCG, which lacks the mannose cap of LAM, suggest its redundant role in IL-10 production in LPS-primed human DCs (Appelmelk et al., 2008). It has been reported that mycobacteria may possess other possible unidentified Dectin-2 ligands, such as mannosylated proteins (Pitarque et al., 2005). These components might account, at least in part, for the IL-10 production induced by whole bacteria.

It has been reported that the IL-10 production during infection correlates with susceptibility to *M. tuberculosis*. Large amounts of IL-10 can be detected in the serum of active tuberculosis patients, particularly in response to hypervirulent strains of *M. tuberculosis* (O'Garra et al., 2013). In line with these observations, increased susceptibility to mycobacteria has been shown in mice that constitutively overexpressed IL-10 (Feng et al., 2002). In addition, secretion of another immune-regulatory cytokine transforming growth factor-β (TGF-β) was also slightly enhanced by Man-LAM through Dectin-2 (data not shown). However, the precise contribution of the mannose cap of LAM to the virulency of mycobacteria still remains controversial in vivo (Afonso-Barroso et al., 2012; Appelmelk et al., 2008).

On the other hand, it has been proposed that IL-10 might limit excessive damage to the host tissue (Redford et al., 2011). The mutant mice lacking CARD9, a downstream adaptor of FcRγ, exhibited severe lung pathology and enhanced lethality in response to *M. tuberculosis*, which is correlated with abolished secretion of IL-10 (Dorhoi et al., 2010). Although CARD9 also mediates signaling through Mincle, the effect of Mincle deficiency on the pathologies during mycobacterial infection was modest compared with those of *CARD9*$^{-/-}$ mice (Behler et al., 2012; Heitmann et al., 2013; Lee et al., 2012). Given the augmented lung inflammation in *Clec4n*$^{-/-}$ mice, the Dectin-2-FcRγ-CARD9 axis appears to be involved in the control of mycobacterial infection. Indeed, *Fcer1g*$^{-/-}$ mice showed increased immunopathology in the lungs during mycobacterial infection (Maglione et al., 2008).

How does Man-LAM efficiently promote Th17 cell responses in mice? A previous study demonstrates that Dectin-2 ligand is

capable of inducing the Th17 cell differentiation through the release of soluble factors (Saijo et al., 2010). Man-LAM stimulation also induced the production of IL-6, TNF, and TGF-β, all of which are Th17-cell-inducing cytokines. In addition, we observed that the transcription of IL-23p19 was upregulated in BMDCs upon Man-LAM in a Dectin-2-dependent fashion (data not shown), as previously reported in BMDCs stimulated with *C. albicans* (Robinson et al., 2009). A recent report has demonstrated that a NTM strain *M. avium* bearing Man-LAM could induce IL-23 production. This activity is lost in the lipophilic extract of the strain (Jönsson et al., 2012), supporting the idea that hydrophilic Man-LAM is involved in the promotion of Th17 cell differentiation.

In human PBMCs from tuberculosis patients, we found that Man-LAM enhanced IFN-γ production induced by mycobacterial antigen. The undetectable concentration of IL-17 secretion (data not shown) is consistent with previous observation (Yamashita et al., 2013), although the underlying mechanism is currently unknown. One possible explanation is that T cells in tuberculosis patients might have already skewed to a Th1 cell phenotype upon repetitive antigen exposure during infection.

In sharp contrast to Mincle ligand TDM, Dectin-2 ligand Man-LAM uniquely induces the production of IL-10 and IL-2, despite the fact that both CLRs share the same signaling subunit FcRγ. IL-2 production from DCs might contribute to the adjuvanticity by promoting T cell priming (Granucci et al., 2001). Previous studies have highlighted the role of Syk-CARD9 pathway in the production of IL-10 and IL-2 in DCs (LeibundGut-Landmann et al., 2007; Robinson et al., 2009; Saijo et al., 2010), because the TLR-MyD88 or TRIF pathway does not lead to secretion of these cytokines (LeibundGut-Landmann et al., 2007). However, the Syk-CARD9 pathway is not sufficient to induce these cytokines, because the Mincle ligand TDM did not allow the production of either IL-10 or IL-2. It remains unclear how distinct CLRs lead to different cellular responses through a common signaling subunit. We previously reported that the quantity and duration of FcRγ signals can determine the quality of cellular responses (Yamasaki et al., 2004). It is intriguing to hypothesize that the kinetics, affinity, or valency of receptor engagement potentially generates distinct signaling through FcRγ.

In addition to the functions of Man-LAM described above, Man-LAM is known to have pleiotropic functions during mycobacterial infection. Mycobacteria limit phagosome-lysosome fusion to survive in macrophages, which allow mycobacteria to establish latent and persistent infection (Pieters, 2008). Man-LAM is one of the candidate involved in this process (Fratti et al., 2003; Vergne et al., 2004), although more detailed studies are needed to determine whether Dectin-2-mediated signaling affects phagosome-lysosome fusion. A recent study has demonstrated that Man-LAM treatment inhibits T cell migration from the draining lymph nodes (Richmond et al., 2012). This effect seems to occur independently of Dectin-2, as its expression was not detected in any subsets of T cells (Ariizumi et al., 2000).

In the present study, we have shown that Dectin-2 recognizes Man-LAM to mediate its adjuvanticity. In addition, the simultaneous induction of both immunostimulatory and inhibitory responses by Man-LAM-Dectin-2 axis might be beneficial for host organisms to maintain balanced immune responses. During EAE development, skin inflammation is observed at the injection site when TDM was used as an adjuvant (Miyake et al., 2013). However, no such inflammation was observed in the skin of Man-LAM-injected mice (data not shown), implying that the anti-inflammatory cytokines induced by Man-LAM might control excessive inflammation at the injection site. The limited inflammatory responses induced by Man-LAM could thus be beneficial as an adjuvant for therapeutic vaccines for infectious diseases and cancer. It is therefore proposed that Man-LAM analogs might represent unique hydrophilic "regulatory" adjuvants that promote the development of acquired immunity, with minimal detrimental inflammation.

EXPERIMENTAL PROCEDURES

Lipids Extract

M. bovis BCG was fractionated by distilled water with repeated washing five times. After centrifugation, the soluble fraction was collected. The insoluble fraction was further delipidated with C:M (2:1, vol/vol). Each fraction was resuspended in a volume of isopropanol at equivalent amount of 0.1 mg as the original *M. bovis* BCG weight.

Cells

2B4-NFAT-GFP reporter cells expressing FcRγ alone, Mincle, Dectin-2, and Dectin-2^{QPD} were prepared as previously described (Yamasaki et al., 2009). BMDCs were prepared as previously described (Miyake et al., 2013).

In Vitro Stimulation

Mycobacterial lipid extracts, LAM in aqueous solution (1 mg/ml), TDM dissolved in C:M at 1 mg/ml, and *Candida albicans* cell wall mannan (5 mg/ml) were diluted in isopropanol and added to 96-well plates at 20 μl/well, followed by evaporation of the solvents as previously described (Ishikawa et al., 2009). Reporter cells were stimulated for 24 hr and the activation of NFAT-GFP was monitored using flow cytometry. BMDCs were stimulated for 2 days, then the culture supernatants were collected. The concentrations of each cytokine were determined by ELISA. Activation was determined using surface staining of the costimulatory molecules CD40 and CD80 by flow cytometry.

OVA-Specific $CD4^+$ T Cell Responses

BMDCs were generated from WT and *Clec4n*$^{-/-}$ mice as described above. BMDCs were left untreated or stimulated with indicated amount of plate-coated LAM in the presence of $OVA_{323-339}$ peptides (ABGENT). $CD4^+$ T cells from OT-II Tg mice were purified with anti-CD4-conjugated magnetic beads (MACS, Miltenyi) and then labeled with CFSE (DOJINDO) and cocultured with OVA-pulsed DCs in 96-well plates. On day 3, the supernatants were harvested and determined the concentration of IFN-γ, IL-17, and IL-10 using ELISA. CFSE-labeled T cells were analyzed for dilution of CFSE within the $CD4^+$ T cell population using flow cytometry.

Experimental Autoimmune Encephalomyelitis

Mice were immunized via subcutaneous administration of 200 μg of MOG_{35-55} peptide (Invitrogen) emulsified in IFA (Difco) containing 500 μg of LAM on day 0. The mice received three daily intraperitoneal (i.p.) administrations of 500 ng of pertussis toxin (PT) (List Biological Laboratories) starting on day 1. The disease severity was scored as previously described (Miyake et al., 2013). For the in vitro restimulation analysis, cells were collected from the axillary, inguinal, and lumbar (paraaortic) lymph nodes on day 23. Lymphocytes (5×10^5 cells/well) were stimulated with MOG_{35-55} peptides at the indicated concentrations for 4 days. The concentrations of IL-17, IFN-γ, and GM-SCF in culture supernatants were determined by ELISA. All animal protocols were approved by the committee of Ethics on Animal Experiment, Faculty of Medical Sciences, Kyushu University, Chiba University, or Tokyo University of Pharmacy and Life Sciences.

Mycobacterial Infection

For in vitro infection, BMDCs were infected with 1 to 10×10^9 CFU of *M. bovis* BCG. After 48 hr, the culture supernatants were collected and cytokine

concentration was determined by ELISA. For in vivo infection, WT mice and *Clec4n*$^{-/-}$ mice were anesthetized with isoflurane, and each mouse was subsequently infected intranasally with 2.5 × 10^6 CFU *M. avium* complex (MAC) per mouse. At 3 weeks after infection, the lungs were isolated and homogenized with a Physcotron handy microhomogenizer (Microtec). Serial dilutions of the homogenates were subjected to the determination of CFU on 7H11 agar plates supplemented with OADC and penicillin (100 U/ml). The homogenates were also subjected to the determination of chemokines with a Cytometric Bead Array System (BD Biosciences). Lungs from other infected mice were fixed with 10% formaldehyde for hematoxylin-eosin staining. Single-cell suspensions of splenocytes (5 × 10^5 cells) were stimulated with *M. avium* sensitin PPD (5 μg/ml) or MAC Ag85A (10 μg/ml) for 4 days, and the concentrations of cytokines and chemokines in culture supernatants were determined by ELISA. Four patients of National Tokyo Hospital in Tokyo, Japan, were enrolled in this study after giving informed consent. The research protocol was approved by the Institutional Review Board of National Tokyo Hospital and by the ethical committee of the National Institute of Infectious Diseases for medical research using human subjects.

SUPPLEMENTAL INFORMATION

Supplemental Information includes six figures and Supplemental Experimental Procedures and can be found with this article online at http://dx.doi.org/10.1016/j.immuni.2014.08.005.

AUTHOR CONTRIBUTIONS

A.Y., S.S., and S.Y. designed the research; A.Y., S.S., Y.H., Y.M., E.I., M.S., and M.Y. did the experiments; H.I., M.T., and K.A. provided the materials; and A.Y., S.S., M.O., and S.Y. wrote the manuscript.

ACKNOWLEDGMENTS

We thank I. Yano, Y. Morita, K. Kawakami, D. Mori, and K. Toyonaga for discussion; S. Akira and T. Saito for providing mice; K. Machida, K. Wakamatsu, and Y. Koreeda for providing NTM strains; T. Kamichi for technical support; Y. Sanui for secretarial assistance; and Laboratory for Technical Support, Medical Institute of Bioregulation, Kyushu University for support. This work was partly performed in the Cooperative Research Project Program of the Medical Institute of Bioregulation, Kyushu University and Medical Mycology Research Center, Chiba University. This work was supported by Funding Program for Next Generation World-Leading Researcher (NEXT Program) and Coordination, Support and Training Program for Translational Research and Grant-in-Aid for Scientific Research from the Japanese Ministry of Education, Culture, Sports, Science, and Technology.

Received: December 25, 2013
Accepted: August 7, 2014
Published: August 28, 2014

REFERENCES

Afonso-Barroso, A., Clark, S.O., Williams, A., Rosa, G.T., Nóbrega, C., Silva-Gomes, S., Vale-Costa, S., Ummels, R., Stoker, N., Movahedzadeh, F., et al. (2012). Lipoarabinomannan mannose caps do not affect mycobacterial virulence or the induction of protective immunity in experimental animal models of infection and have minimal impact on in vitro inflammatory responses. Cell. Microbiol. *15*, 660–674.

Appelmelk, B.J., den Dunnen, J., Driessen, N.N., Ummels, R., Pak, M., Nigou, J., Larrouy-Maumus, G., Gurcha, S.S., Movahedzadeh, F., Geurtsen, J., et al. (2008). The mannose cap of mycobacterial lipoarabinomannan does not dominate the *Mycobacterium*-host interaction. Cell. Microbiol. *10*, 930–944.

Ariizumi, K., Shen, G.L., Shikano, S., Ritter, R., 3rd, Zukas, P., Edelbaum, D., Morita, A., and Takashima, A. (2000). Cloning of a second dendritic cell-associated C-type lectin (dectin-2) and its alternatively spliced isoforms. J. Biol. Chem. *275*, 11957–11963.

Behler, F., Steinwede, K., Balboa, L., Ueberberg, B., Maus, R., Kirchhof, G., Yamasaki, S., Welte, T., and Maus, U.A. (2012). Role of Mincle in alveolar macrophage-dependent innate immunity against mycobacterial infections in mice. J. Immunol. *189*, 3121–3129.

Belanger, A.E., Besra, G.S., Ford, M.E., Mikusová, K., Belisle, J.T., Brennan, P.J., and Inamine, J.M. (1996). The *embAB* genes of *Mycobacterium avium* encode an arabinosyl transferase involved in cell wall arabinan biosynthesis that is the target for the antimycobacterial drug ethambutol. Proc. Natl. Acad. Sci. USA *93*, 11919–11924.

Briken, V., Porcelli, S.A., Besra, G.S., and Kremer, L. (2004). Mycobacterial lipoarabinomannan and related lipoglycans: from biogenesis to modulation of the immune response. Mol. Microbiol. *53*, 391–403.

Chan, E.D., Morris, K.R., Belisle, J.T., Hill, P., Remigio, L.K., Brennan, P.J., and Riches, D.W. (2001). Induction of inducible nitric oxide synthase-NO* by lipoarabinomannan of *Mycobacterium tuberculosis* is mediated by MEK1-ERK, MKK7-JNK, and NF-kappaB signaling pathways. Infect. Immun. *69*, 2001–2010.

Dorhoi, A., Desel, C., Yeremeev, V., Pradl, L., Brinkmann, V., Mollenkopf, H.J., Hanke, K., Gross, O., Ruland, J., and Kaufmann, S.H. (2010). The adaptor molecule CARD9 is essential for tuberculosis control. J. Exp. Med. *207*, 777–792.

Drickamer, K. (1992). Engineering galactose-binding activity into a C-type mannose-binding protein. Nature *360*, 183–186.

Feng, C.G., Kullberg, M.C., Jankovic, D., Cheever, A.W., Caspar, P., Coffman, R.L., and Sher, A. (2002). Transgenic mice expressing human interleukin-10 in the antigen-presenting cell compartment show increased susceptibility to infection with *Mycobacterium avium* associated with decreased macrophage effector function and apoptosis. Infect. Immun. *70*, 6672–6679.

Fratti, R.A., Chua, J., Vergne, I., and Deretic, V. (2003). *Mycobacterium tuberculosis* glycosylated phosphatidylinositol causes phagosome maturation arrest. Proc. Natl. Acad. Sci. USA *100*, 5437–5442.

Geijtenbeek, T.B., Van Vliet, S.J., Koppel, E.A., Sanchez-Hernandez, M., Vandenbroucke-Grauls, C.M., Appelmelk, B., and Van Kooyk, Y. (2003). Mycobacteria target DC-SIGN to suppress dendritic cell function. J. Exp. Med. *197*, 7–17.

Granucci, F., Vizzardelli, C., Pavelka, N., Feau, S., Persico, M., Virzi, E., Rescigno, M., Moro, G., and Ricciardi-Castagnoli, P. (2001). Inducible IL-2 production by dendritic cells revealed by global gene expression analysis. Nat. Immunol. *2*, 882–888.

Gringhuis, S.I., den Dunnen, J., Litjens, M., van Het Hof, B., van Kooyk, Y., and Geijtenbeek, T.B. (2007). C-type lectin DC-SIGN modulates Toll-like receptor signaling via Raf-1 kinase-dependent acetylation of transcription factor NF-kappaB. Immunity *26*, 605–616.

Gringhuis, S.I., den Dunnen, J., Litjens, M., van der Vlist, M., and Geijtenbeek, T.B. (2009). Carbohydrate-specific signaling through the DC-SIGN signalosome tailors immunity to *Mycobacterium tuberculosis*, HIV-1 and *Helicobacter pylori*. Nat. Immunol. *10*, 1081–1088.

Heitmann, L., Schoenen, H., Ehlers, S., Lang, R., and Hölscher, C. (2013). Mincle is not essential for controlling *Mycobacterium tuberculosis* infection. Immunobiology *218*, 506–516.

Ishikawa, E., Ishikawa, T., Morita, Y.S., Toyonaga, K., Yamada, H., Takeuchi, O., Kinoshita, T., Akira, S., Yoshikai, Y., and Yamasaki, S. (2009). Direct recognition of the mycobacterial glycolipid, trehalose dimycolate, by C-type lectin Mincle. J. Exp. Med. *206*, 2879–2888.

Ishikawa, T., Itoh, F., Yoshida, S., Saijo, S., Matsuzawa, T., Gonoi, T., Saito, T., Okawa, Y., Shibata, N., Miyamoto, T., and Yamasaki, S. (2013). Identification of distinct ligands for the C-type lectin receptors Mincle and Dectin-2 in the pathogenic fungus *Malassezia*. Cell Host Microbe *13*, 477–488.

Jönsson, B., Ridell, M., and Wold, A.E. (2012). Non-tuberculous mycobacteria and their surface lipids efficiently induced IL-17 production in human T cells. Microbes Infect. *14*, 1186–1195.

Józefowski, S., Sobota, A., Pawłowski, A., and Kwiatkowska, K. (2011). *Mycobacterium tuberculosis* lipoarabinomannan enhances LPS-induced

TNF-α production and inhibits NO secretion by engaging scavenger receptors. Microb. Pathog. *50*, 350–359.

Koppel, E.A., Ludwig, I.S., Hernandez, M.S., Lowary, T.L., Gadikota, R.R., Tuzikov, A.B., Vandenbroucke-Grauls, C.M., van Kooyk, Y., Appelmelk, B.J., and Geijtenbeek, T.B. (2004). Identification of the mycobacterial carbohydrate structure that binds the C-type lectins DC-SIGN, L-SIGN and SIGNR1. Immunobiology *209*, 117–127.

Lee, W.B., Kang, J.S., Yan, J.J., Lee, M.S., Jeon, B.Y., Cho, S.N., and Kim, Y.J. (2012). Neutrophils promote mycobacterial trehalose dimycolate-induced lung inflammation via the Mincle pathway. PLoS Pathog. *8*, e1002614.

LeibundGut-Landmann, S., Gross, O., Robinson, M.J., Osorio, F., Slack, E.C., Tsoni, S.V., Schweighoffer, E., Tybulewicz, V., Brown, G.D., Ruland, J., and Reis e Sousa, C. (2007). Syk- and CARD9-dependent coupling of innate immunity to the induction of T helper cells that produce interleukin 17. Nat. Immunol. *8*, 630–638.

Leopold, K., and Fischer, W. (1993). Molecular analysis of the lipoglycans of *Mycobacterium tuberculosis*. Anal. Biochem. *208*, 57–64.

Maglione, P.J., Xu, J., Casadevall, A., and Chan, J. (2008). Fc γ receptors regulate immune activation and susceptibility during *Mycobacterium tuberculosis* infection. J. Immunol. *180*, 3329–3338.

Mazurek, J., Ignatowicz, L., Kallenius, G., Svenson, S.B., Pawlowski, A., and Hamasur, B. (2012). Divergent effects of mycobacterial cell wall glycolipids on maturation and function of human monocyte-derived dendritic cells. PLoS ONE *7*, e42515.

McGreal, E.P., Rosas, M., Brown, G.D., Zamze, S., Wong, S.Y., Gordon, S., Martinez-Pomares, L., and Taylor, P.R. (2006). The carbohydrate-recognition domain of Dectin-2 is a C-type lectin with specificity for high mannose. Glycobiology *16*, 422–430.

Mishra, A.K., Driessen, N.N., Appelmelk, B.J., and Besra, G.S. (2011). Lipoarabinomannan and related glycoconjugates: structure, biogenesis and role in *Mycobacterium tuberculosis* physiology and host-pathogen interaction. FEMS Microbiol. Rev. *35*, 1126–1157.

Miyake, Y., Toyonaga, K., Mori, D., Kakuta, S., Hoshino, Y., Oyamada, A., Yamada, H., Ono, K.I., Suyama, M., Iwakura, Y., et al. (2013). C-type lectin MCL is an FcRγ-coupled receptor that mediates the adjuvanticity of mycobacterial cord factor. Immunity *38*, 1050–1062.

Nagaoka, K., Takahara, K., Minamino, K., Takeda, T., Yoshida, Y., and Inaba, K. (2010). Expression of C-type lectin, SIGNR3, on subsets of dendritic cells, macrophages, and monocytes. J. Leukoc. Biol. *88*, 913–924.

Nigou, J., Zelle-Rieser, C., Gilleron, M., Thurnher, M., and Puzo, G. (2001). Mannosylated lipoarabinomannans inhibit IL-12 production by human dendritic cells: evidence for a negative signal delivered through the mannose receptor. J. Immunol. *166*, 7477–7485.

O'Garra, A., Redford, P.S., McNab, F.W., Bloom, C.I., Wilkinson, R.J., and Berry, M.P. (2013). The immune response in tuberculosis. Annu. Rev. Immunol. *31*, 475–527.

Pieters, J. (2008). *Mycobacterium tuberculosis* and the macrophage: maintaining a balance. Cell Host Microbe *3*, 399–407.

Pitarque, S., Herrmann, J.L., Duteyrat, J.L., Jackson, M., Stewart, G.R., Lecointe, F., Payre, B., Schwartz, O., Young, D.B., Marchal, G., et al. (2005). Deciphering the molecular bases of *Mycobacterium tuberculosis* binding to the lectin DC-SIGN reveals an underestimated complexity. Biochem. J. *392*, 615–624.

Redford, P.S., Murray, P.J., and O'Garra, A. (2011). The role of IL-10 in immune regulation during *M. tuberculosis* infection. Mucosal Immunol. *4*, 261–270.

Richmond, J.M., Lee, J., Green, D.S., Kornfeld, H., and Cruikshank, W.W. (2012). Mannose-capped lipoarabinomannan from *Mycobacterium tuberculosis* preferentially inhibits sphingosine-1-phosphate-induced migration of Th1 cells. J. Immunol. *189*, 5886–5895.

Robinson, M.J., Osorio, F., Rosas, M., Freitas, R.P., Schweighoffer, E., Gross, O., Verbeek, J.S., Ruland, J., Tybulewicz, V., Brown, G.D., et al. (2009). Dectin-2 is a Syk-coupled pattern recognition receptor crucial for Th17 responses to fungal infection. J. Exp. Med. *206*, 2037–2051.

Saijo, S., Ikeda, S., Yamabe, K., Kakuta, S., Ishigame, H., Akitsu, A., Fujikado, N., Kusaka, T., Kubo, S., Chung, S.H., et al. (2010). Dectin-2 recognition of α-mannans and induction of Th17 cell differentiation is essential for host defense against *Candida albicans*. Immunity *32*, 681–691.

Sato, K., Yang, X.L., Yudate, T., Chung, J.S., Wu, J., Luby-Phelps, K., Kimberly, R.P., Underhill, D., Cruz, P.D., Jr., and Ariizumi, K. (2006). Dectin-2 is a pattern recognition receptor for fungi that couples with the Fc receptor γ chain to induce innate immune responses. J. Biol. Chem. *281*, 38854–38866.

Schlesinger, L.S., Hull, S.R., and Kaufman, T.M. (1994). Binding of the terminal mannosyl units of lipoarabinomannan from a virulent strain of *Mycobacterium tuberculosis* to human macrophages. J. Immunol. *152*, 4070–4079.

Tailleux, L., Schwartz, O., Herrmann, J.L., Pivert, E., Jackson, M., Amara, A., Legres, L., Dreher, D., Nicod, L.P., Gluckman, J.C., et al. (2003). DC-SIGN is the major *Mycobacterium tuberculosis* receptor on human dendritic cells. J. Exp. Med. *197*, 121–127.

Tanne, A., Ma, B., Boudou, F., Tailleux, L., Botella, H., Badell, E., Levillain, F., Taylor, M.E., Drickamer, K., Nigou, J., et al. (2009). A murine DC-SIGN homologue contributes to early host defense against *Mycobacterium tuberculosis*. J. Exp. Med. *206*, 2205–2220.

Torrelles, J.B., Azad, A.K., and Schlesinger, L.S. (2006). Fine discrimination in the recognition of individual species of phosphatidyl-myo-inositol mannosides from *Mycobacterium tuberculosis* by C-type lectin pattern recognition receptors. J. Immunol. *177*, 1805–1816.

Vergne, I., Chua, J., Singh, S.B., and Deretic, V. (2004). Cell biology of *mycobacterium tuberculosis* phagosome. Annu. Rev. Cell Dev. Biol. *20*, 367–394.

Wieland, C.W., Koppel, E.A., den Dunnen, J., Florquin, S., McKenzie, A.N., van Kooyk, Y., van der Poll, T., and Geijtenbeek, T.B. (2007). Mice lacking SIGNR1 have stronger T helper 1 responses to *Mycobacterium tuberculosis*. Microbes Infect. *9*, 134–141.

Yamasaki, S., Ishikawa, E., Kohno, M., and Saito, T. (2004). The quantity and duration of FcRgamma signals determine mast cell degranulation and survival. Blood *103*, 3093–3101.

Yamasaki, S., Matsumoto, M., Takeuchi, O., Matsuzawa, T., Ishikawa, E., Sakuma, M., Tateno, H., Uno, J., Hirabayashi, J., Mikami, Y., et al. (2009). C-type lectin Mincle is an activating receptor for pathogenic fungus, *Malassezia*. Proc. Natl. Acad. Sci. USA *106*, 1897–1902.

Yamashita, Y., Hoshino, Y., Oka, M., Matsumoto, S., Ariga, H., Nagai, H., Makino, M., Ariyoshi, K., and Tsunetsugu-Yokota, Y. (2013). Multicolor flow cytometric analyses of $CD4^+$ T cell responses to *Mycobacterium tuberculosis*-related latent antigens. Jpn. J. Infect. Dis. *66*, 207–215.

Zhu, L.L., Zhao, X.Q., Jiang, C., You, Y., Chen, X.P., Jiang, Y.Y., Jia, X.M., and Lin, X. (2013). C-type lectin receptors Dectin-3 and Dectin-2 form a heterodimeric pattern-recognition receptor for host defense against fungal infection. Immunity *39*, 324–334.

Clinical Immunology (2014) 153, 64–72

available at www.sciencedirect.com

Clinical Immunology

www.elsevier.com/locate/yclim

Involvement of mannose-binding lectin in the pathogenesis of Kawasaki disease-like murine vasculitis

Akihiro Nakamura [a,*], Mitsuhiko Okigaki [b], Noriko Miura [c], Chinatsu Suzuki [a], Naohito Ohno [c], Fuyuki Kametani [d], Kenji Hamaoka [a]

[a] *Department of Pediatric Cardiology and Nephrology, Graduate School of Medical Science, Kyoto Prefectural University of Medicine, 465 Kajii-Cyo, Hirokouji, Kawaramachi dori, Kamigyo-ku, Kyoto City 602-8566, Japan*
[b] *Department of Cardiology and Nephrology, Graduate School of Medical Science, Kyoto Prefectural University of Medicine, 465 Kajii-Cyo, Hirokouji, Kawaramachi dori, Kamigyo-ku, Kyoto City 602-8566, Japan*
[c] *Laboratory for Immunopharmacology of Microbial Products, School of Pharmacy, Tokyo University of Pharmacy and Life Sciences, 1432-1 Horinouchi, Hachioji, Tokyo 192-0392, Japan*
[d] *Department of Dementia and Higher Brain Function, Tokyo Metropolitan Institute of Medical Science, 2-1-6 Kamikitazawa, Setagaya-ku, Tokyo 156-8506, Japan*

Received 28 January 2014; accepted with revision 28 March 2014
Available online 8 April 2014

KEYWORDS
Kawasaki disease;
Vasculitis;
Mannose-binding lectin;
Animal model

Abstract Kawasaki disease (KD) is a paediatric idiopathic vasculitis. In this study, on the basis of studies using an established animal model for KD, we report that mannose-binding lectin (MBL) is involved in the pathogenesis of the disease. KD-like experimental murine vasculitis was induced by intraperitoneally administering a *Candida albicans* water-soluble extract (CAWS). MBL-A gradually increased in the serum of the model mice treated with CAWS. Deposition of MBL-A and MBL-C was observed in the aortic root, including the coronary arteries, which is a predilection site in experimental vasculitis. Corresponding to the distribution patterns of MBLs, marked deposition of C3/C3-derived peptides was also observed. Regarding the self-reactivity of MBLs, we observed that MBLs interacted with core histones to activate the lectin pathway. These results suggest that some types of pathogens provoke the MBL-dependent complement pathway (lectin pathway) to cause and/or exacerbate KD-like vasculitis.

1. Introduction

Kawasaki disease (KD) is a paediatric idiopathic vasculitis, which can sometimes result in aneurysms of the coronary arteries [1], leading to an increased risk of myocardial infarction [2]. Although its molecular pathogenesis is still

* Corresponding author.
E-mail address: nakam993@koto.kpu-m.ac.jp (A. Nakamura).

http://dx.doi.org/10.1016/j.clim.2014.03.019
1521-6616/

unclear, a line of studies has suggested that an uncontrolled immune response to infectious stimuli is involved in the pathogenesis of KD [3].

In particular, many investigators have reported a possible relationship between KD and superantigens [4–6], which are pathogen-derived substances that activate a specific class of T cells and induce massive production of cytokines [7]. For example, Yoshioka et al. reported that Vβ2/Vβ6.5 T cells, which are responsive to *Streptococcus*-derived pyrogenic exotoxin C, are increased in KD patients [8,9]. Although superantigens have been considered one of the most likely causal factors of KD [10], some studies do not support this hypothesis [6,11,12].

Compared with cellular immunity, little is known about the role(s) of innate humoral immunity in the pathogenesis of KD. However, some population genetic studies have reported a possible relationship between KD and genetic polymorphisms of mannose-binding lectin (MBL) [13–16], a circulating pattern recognition receptor protein, which recognises particular carbohydrate structures in microorganisms to activate the complement pathway (lectin pathway) [17]. The MBL genotype affects the plasma levels of MBL. In KD patients younger than 1 year middle/low MBL-expressing genotype increases the risk of coronary artery lesion (CAL) formation, whereas high MBL-expressing genotype increases the risk of CAL in KD patients older than 1 year [14,15]. These findings suggest that CAL susceptibility is not simply a result of a deficiency of the MBL-dependent innate immune system in response to pathogens, implying that the adverse effects of MBL should also be taken into consideration. In fact, MBL has been implicated in a number of diseases, including rheumatic heart disease, rheumatoid arthritis and ischemia–reperfusion injury [18–20]. However, with the exception of ischemia–reperfusion injury, the pathophysiological roles of MBL remain elusive in these diseases, including KD.

Because limited clinical specimens (e.g. blood and urine) are available for the study of KD, animal models are indispensable tools to investigate the molecular mechanisms underlying the disease. *Candida albicans* water-soluble extract (CAWS)-induced murine vasculitis is one of the most established animal models for KD [21], and it shares pathological features with KD [22]. Although the molecular basis underlying the experimental KD-like vasculitis is unclear, understanding its pathological mechanisms is important for elucidating the aetiology of KD.

In the present study, we employed a KD animal model to investigate the involvement of MBL in the pathogenesis of KD-like murine vasculitis. On the basis of the results, we report that the MBL-dependent complement pathway is involved in the pathological processes of KD-like experimental vasculitis.

2. Materials and methods

2.1. Animals

Male DBA/2CrSlc mice (4–5 weeks old) were used throughout this study. Mice were provided by Shimizu Experimental Materials Co., Ltd. and used in the experimental animal facility of the Kyoto Prefectural University of Medicine. The animal experiments were conducted in accordance with the university's guidelines for experimental animal studies. CAWS was prepared as described in [23]. The murine vasculitis model was prepared by the method established by Ohno and Nagi-Miura et al. [21,23]. In brief, mice were intraperitoneally administered CAWS [1 mg/(mouse·day)] or PBS (sham control group) for 5 days. Mice were then euthanised under general anaesthesia on day 1, 6 or 11 after CAWS administration for 5 consecutive days.

2.2. Pathological study

Four mice per experimental group were used. After washing the blood out by perfusion with PBS(−), the organs were excised and immediately frozen in OTC compound without fixation. The specimens were sectioned using a cryostat to generate 8-μm sections. Immunohistochemical detection was conducted according to the manufacturer's instructions. For the detection of MBL-C, sections were fixed with acetone for 10 min. After incubation in 0.3% hydrogen peroxide/methanol for 20 min, the sections were washed with TBS and then blocked with 10% goat serum-PBS (Nichirei, Tokyo) for 15 min. The sections were incubated with an anti-MBL-C rat monoclonal antibody (1:25 dilution) (HyCult, Uden) in TBS/0.02% Tween20 [TBS-T] containing 3% BSA and 1 mM $CaCl_2$ at room temperature (RT) for 2 h. After

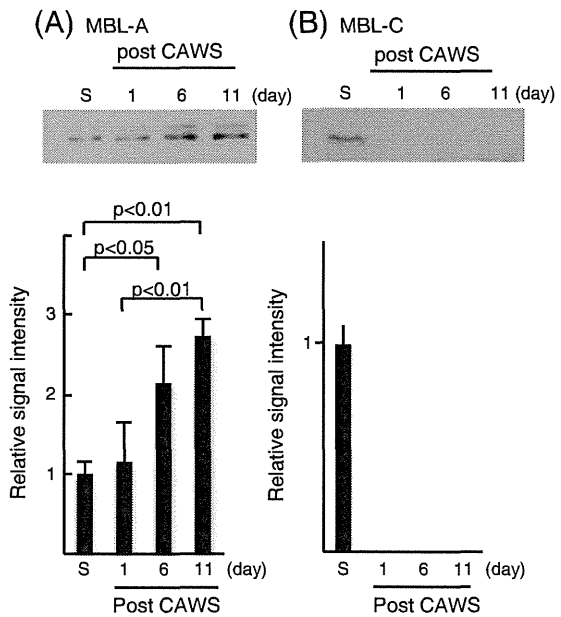

Figure 1 *Candida albicans* water-soluble extract (CAWS)-induced quantitative changes in serum mannose-binding lectin (MBL)-A and -C levels. Time-dependent quantitative changes of (A) MBL-A and (B) MBL-C in the serum of CAWS-treated mice were determined using western blotting. Electrophoresis for MBL-A was performed under non-reducing conditions. The signal intensity of each group was quantified and is shown as mean ± standard deviation (n = 3/group). 'S' stands for serum from the sham control mice. Signal intensities are shown as relative values compared with the sham control. Representative immunoblots are shown at the top of the figure.

washing with TBS containing 1 mM $CaCl_2$ [TBS-Ca], they were subsequently incubated with HRP-conjugated anti-rat immunoglobulin G (IgG) antibody (1:1000 dilution) (ab7097; Abcam, Cambridge) at RT for 1 h. After washing with TBS-Ca, the signals were developed using a diaminobenzidine (DAB)-plus substrate kit (DAKO, Glostrup). The reaction was terminated with tap water, and the sections were counterstained with haematoxylin.

Sections for the immunohistochemical study of MBL-A and C3d/C3 were fixed with 4% paraformaldehyde (PFA)/PBS for

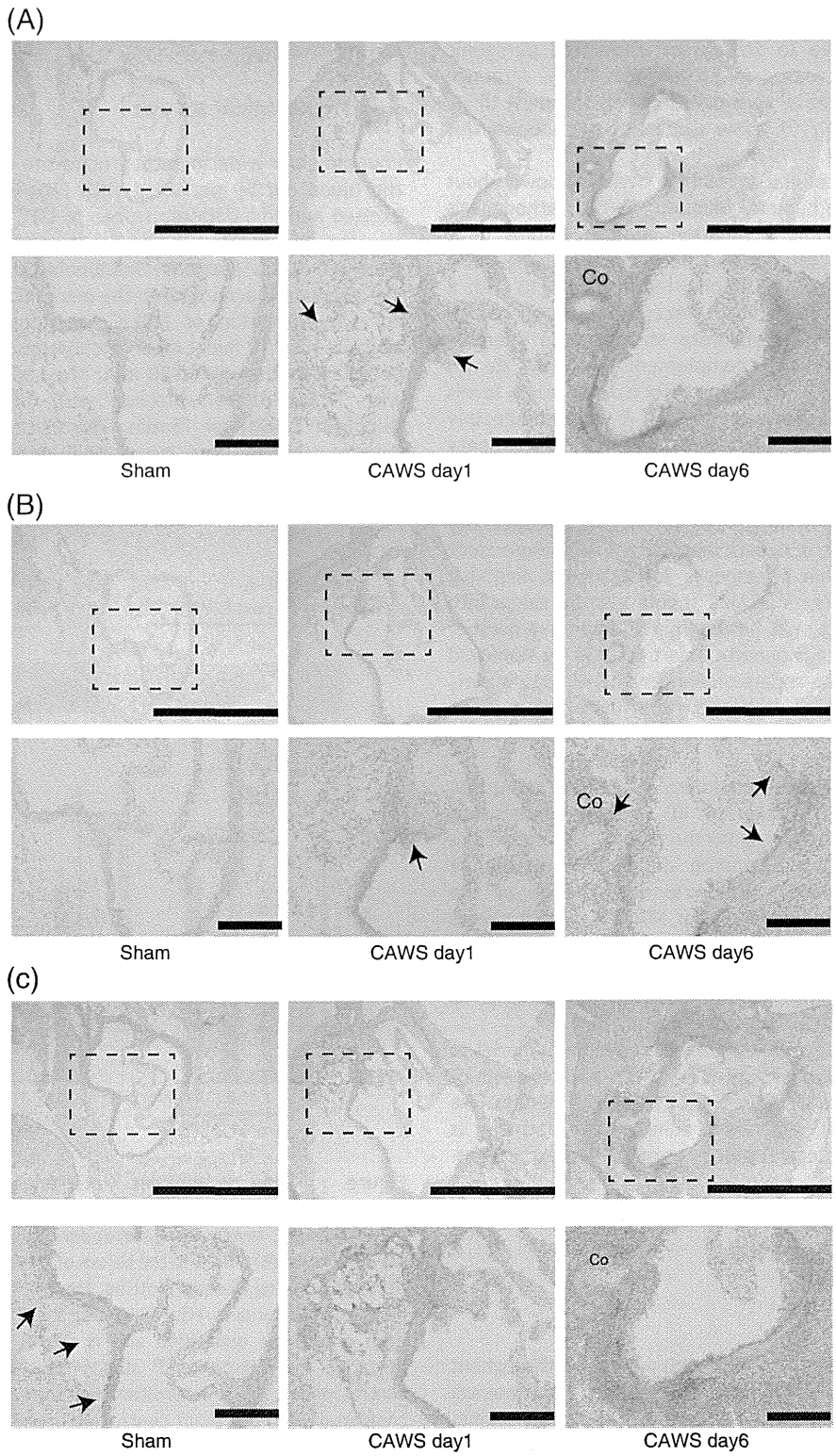

30 min at RT, followed by treatment with 0.3% hydrogen peroxide/methanol for 20 min. After washing with TBS, the specimens were blocked with 10% goat serum/PBS (for MBL-A) or 3% BSA/PBS-T (for C3d/C3) for 15 min. MBL-A was detected by incubating with an anti-MBL-A antibody (1:25 dilution) (HyCult, Uden) in TBS-T containing 1mM $CaCl_2$ at RT for 2 h. Detection of C3/C3d was performed by incubating the sections with an anti-C3d antibody (1:2500) (DAKO, Uden) in 3% BSA/PBS-T at RT for 1 h. After washing with Ca-TBS (for MBL-A) or PBS (for C3d/C3), the sections were incubated with a HRP-labelled anti-rat IgG antibody (1: 1,000 dilution) (ab7097, Abcam, Cambridge) in 3% BSA / Ca-TBS-T (for MBL-A) for 1h or a HRP-labelled anti-rabbit IgG antibody (ab80437, Abcam, Cambridge) (for C3/C3d) at RT for 10 min. After washing, the signals were developed with DAB plus a substrate Chromogen system (DAKO, Uden). The reaction was terminated with tap water, and the sections were counterstained with haematoxylin. Normal rat or rabbit IgG was used as negative control for immunostaining.

For the immunohistochemical detection of IgM, the frozen sections were fixed with 4% PFA/PBS for 30 min, followed by treatment with 0.3% hydrogen peroxide/methanol for 20 min. After washing with PBS, the sections were blocked with 10% goat serum/PBS (Nichirei, Tokyo). Subsequently, the sections were incubated with a HRP-labelled anti-mouse IgM antibody (1:1000 dilution) (Abcam, Cambridge) at RT for 2 h. After washing with PBS, the signals were developed with DAB plus a substrate Chromogen system (DAKO, Uden). The reaction was terminated with tap water, and the sections were counterstained with haematoxylin.

2.3. Biochemical study

Murine serum was diluted (1:100) with Laemmli's buffer and then subjected to immunoblotting with rat monoclonal antibodies against MBL-A (HyCult, Uden) or MBL-C (HyCult, Uden) in the presence of 1 mM $CaCl_2$. Immunodetection was performed with a HRP-labeled anti-rat IgG antibody and enhanced chemiluminescence (ECL) kit (GE Healthcare, Buckinghamshire). Signals derived from endogenous IgG were distinguished from MBL-A and -C signals on the immunoblot by omitting primary antibodies.

To explore endogenous targets for MBL, the blot was blocked with 3% BSA/PBS-T and then probed with 0.2 μg/mL recombinant mouse MBL-C or MBL-A (R&D, NE) in the same buffer containing 1 mM $CaCl_2$ at RT for 1 h with gentle agitation. A hybrid back was not used for avoiding increased background staining. In some cases, the incubation was carried out in the presence of yeast mannan (Tokyo Kasei, Tokyo). After extensive washing with PBS-T containing 3% BSA and 1 mM $CaCl_2$, the blot was incubated with an anti-MBL-A or MBL-C antibody in the same buffer containing 1 mM $CaCl_2$ at 4 °C overnight. Immunodetection was performed as described above.

Purification and analysis of acid-soluble proteins were performed as previously reported [24] with some modifications. In brief, the aortic tissue was homogenised and then washed 3 times in TBS buffer containing 1% CHAPS and proteinase inhibitors. The resulting insoluble materials were re-suspended in 0.2 M H_2SO_4 and left on ice for 2 h. After centrifugation, the supernatant was carefully removed and diluted 20-fold with cold ethanol. The mixture was kept at −30 °C overnight. After centrifugation at 12,000 ×*g* for 10 min, the pellet (histone-enriched fraction) was subjected to acid–urea–Triton gel/SDS gel 2-dimensional polyacrylamide gel electrophoresis (AUT/SDS-PAGE) analysis. After far-western blotting, the blot was stained with Coomassie Brilliant Blue G-250. Protein spots relative to the protein of interest were cut out from a gel run in parallel and then subjected to in-gel trypsin digestion, followed by liquid chromatography–ion trap mass spectrometry (LC–MS/MS) analysis as previously reported [25]. MS data were processed by a Mascot search (Supplementary data 1). For the in vitro complement activation assay, highly pure histones were prepared from the mouse liver essentially as previously described [24].

2.4. Activation of the MBL-dependent lectin pathway in vitro

Histones purified from the mouse liver (0.2 μg/well) were covalently immobilised on a 96-well plate using the Takara Peptide Coating Kit (Takara Bio, Shiga), as described in the manufacturer's instructions. After blocking, the wells were washed thrice with water to remove any substance, which would interfere with the assay. Activation of the MBL-dependent lectin pathway was examined using the Complement System Screen Wieslab kit (Euro Diagnostica, Malmo) with some modifications as previously reported [26]. In brief, MBL-standard normal human serum (BioPorto Diagnostics, Gentofte), MBL-deficient human serum (from a B/B genotype donor) (BioPorto Diagnostics, Gentofte) and negative control human serum (Euro Diagnostica, Malmo) were diluted in a MBL assay buffer and then added to the histone-immobilised wells.

The plate was incubated at 37 °C for 70 min and subsequently washed. An alkaline phosphatase-conjugated antibody was added to the membrane attack complex (MAC) and the plate was incubated for 30 min at RT. Signals were developed by incubating the substrate at approximately 23 °C for 60 min, and the absorbance was measured at 405 nm using the Multiscan JX (Thermo, MA).

Figure 2 Immunohistochemical detection of mannose-binding lectin (MBL)-A, MBL-C and C3/C3-derived peptides in the aortic root. Sequential frozen sections of aortic root were subjected to immunohistochemistry with antibodies against (A) MBL-A, (B) MBL-C and (C) C3d, followed by counterstaining with haematoxylin. The left, middle and right panels show the aortic tissues of sham control and post-*Candida albicans* water-soluble extract (CAWS) day 1 and 6 mice, respectively. The upper panels are low-power images of the immunostained aortic root. Scale bar equals 1000 (upper panels) and 200 μm (lower panels). The area in the dotted lines was magnified and is shown in the lower panels. '*Co*' indicates the coronary artery. Four mice per experimental group were used and representative data are shown here.

2.5. Statistical analysis

The quantitative results are shown as means ± standard deviation. Statistical significance was evaluated using the Tukey's multiple comparison method or using unpaired *t*-tests with the StatMate III software (ATMS, Tokyo).

3. Results

3.1. CAWS-induced changes in serum levels of MBL-A and MBL-C

We first determined the changes in the serum levels of MBL. Unlike humans, mice have 2 distinct MBL genes, i.e. *mbl-a* and *mbl-c*. Serum MBL-A levels gradually increased in the CAWS-administered mice, and the levels increased to 2-fold higher than that of control mice by day 6 post-CAWS administration (Fig. 1A). In contrast, serum MBL-C levels rapidly decreased by day 1 in CAWS-treated mice and did not return to normal levels for 11 days (Fig. 1B). However, a marked accumulation of MBL-C was observed in the spleen (Supplemental data 2), indicating that the rapid disappearance of plasma MBL-C may have resulted from changes in its somatic distribution response to CAWS administration.

3.2. Deposition of MBLs in the aortic root

To determine whether the MBL-dependent complementary pathway participates in the inflammation process of CAWS-induced vasculitis, we investigated the distribution of MBLs and C3-derived peptides by immunohistochemistry of the aortic root, which is one of the most susceptible sites for experimental vasculitis, in normal and CAWS-administered mice. Because different experimental conditions were required to detect each molecule and auto-fluorescence of the aorta was unavoidable, we performed the study using sequential tissue sections by employing a substrate-chromogen method instead of performing multiple immunofluorescence staining. Diffuse deposition of MBL-A was detectable in a part of the intima and adventitia of the annuloaortic region on day 1 in CAWS-treated mice (Fig. 2A, middle panels). In contrast, the deposition of MBL-C was more restricted to the intima of the base of the aortic valves (Fig. 2B, arrows). Marked infiltration of neutrophils was observed in the aortic root on day 6 (data not shown). Consistent with this cellular infiltration, a marked deposition of MBL-A was observed in the aortic intima, adventitia, base of the aortic valves and coronary arteries ('*Co*' in Fig. 2) on day 6 in the CAWS-treated mice (Fig. 2A, right panels). However, MBL-C deposition was still restricted to the intima of the annuloaortic region and a part of the coronary arteries on day 6 (Fig. 2B, right panels, arrows). In the sham group (control), the depositions of MBL-A and MBL-C were barely detectable (Figs. 2A–C, left panels).

As KD is so, CAWS-induced vasculitis preferentially affects some specific sites of arteries such as the aortic root, including the coronary ostium [22]. Therefore, we compared the MBL deposition between the aortic root and abdominal aorta. As shown in Supplementary data 3 the deposition of neither MBL-A nor MBL-C was observed in the abdominal aorta, which is less affected in CAWS-induced vasculitis, confirming that the deposition of MBLs was relevant to the vasculitis.

It has been well established that MBL activates complement pathways, resulting in inflammation. Because DBA2 mice are deficient in C5, it was thought that complement-related inflammation may be mediated by intermediate fragments of the complement pathways, such as C3a, C3b, C3d or C4b, without the formation of MAC. Therefore, we investigated the deposition of C3-derived peptides in the tissues. As expected, on day 6 after treatment with CAWS, C3-derived peptides were deposited in the intima, the adventitia and around the aortic root, including the coronary arteries (Fig. 2C, middle and right panels). Considering that the deposition sites were roughly identical to the sites involved in the deposition of MBLs (Fig. 2), MBLs are likely to provoke complement activation at these locations. Although weak signals of C3/C3-derived peptides were detected in the adventitia of control mice (Fig. 2C, left panels, arrows), as reported previously [27], the intensity was much less than that observed in the CAWS-treated mice.

Besides the lectin pathway, it is an intriguing issue if other complement pathways (e.g. classical and alternative pathways) are involved in the vasculitis. In ischemia-related pathogenesis such as myocardial infarction, for example, the classical pathway has been reported to co-operate with the lectin pathway to exacerbate the tissue damage [28,29]. To address the possible implication of the classical pathway in CAWS vasculitis, the deposition of IgM, which is well-known to activate the classical pathway more effectively than IgG, was immunohistochemically investigated. As shown in Supplementary data 4, the marked deposition of IgM was observed in the endothelium and adventitia of the aortic root of CAWS-treated mice, suggesting that IgM-dependent activation of the classical pathway could also, at least in part, be responsible for the vasculitis in co-operation with the lectin pathway.

3.3. Exploration of endogenous targets for MBLs

To elucidate the molecular mechanisms underlying the deposition of MBLs in the inflamed tissue, we explored the possibility of endogenous protein targets for MBLs by a far-western blotting analysis. Aortic tissue extracts from CAWS-treated mice were subjected to the far-western blotting analysis using recombinant mouse MBL-A and MBL-C proteins as probes. As shown in Fig. 3, both MBL-A and MBL-C recognised some specific proteins, including proteins with a molecular weight of approximately 10–15 kDa and high molecular mass proteins (>250 kDa) in the aorta lysates. Incubation of the blot with MBLs in the presence of excess mannan (0.2 mg/mL) markedly diminished the intensity of these signals (Fig. 3A), indicating that recognition took place through the carbohydrate recognition domain of the MBLs.

Using the sequential fractionation of the aortic tissue proteins, the MBL-reactive 10–15-kDa proteins were found to reside in the acid-soluble protein fraction, which is well-known for being enriched in histones (Fig. 3B). This fraction was subsequently subjected to AUT/SDS-PAGE (see Materials and methods), followed by

the far-western blotting or LC–/MS/MS analysis. The 10–15-kDa proteins were eventually identified as histones H4, H2B-type 1H, H3.1 and H2A-type 2A (Fig. 3C; Supplementary material 1), suggesting that these core histone components are potential endogenous targets for MBLs. Because of the low-transfer efficiency of histone H2A, it was unclear whether other H2A subtypes were also preferentially recognised by MBLs.

3.4. Histones and lectin pathway activation

To evaluate whether histones can activate the lectin pathway, highly purified histones (Fig. 4A) were subjected to an in vitro MBL pathway activation assay with normal and MBL-deficient (genotype B/B) human sera. As shown in Fig. 4B, the purified histones significantly activated the MBL-dependent lectin pathway in vitro. However, the activation potential was much less than that of CAWS (data not shown), which is a potent activator of the lectin pathway [26]. To avoid any unidentified artefacts arising from medications, including the intravenous immunoglobulin (IVIG) therapy, and disease-related changes in the complement pathway-related proteins, we did not use sera from KD patients for this assay.

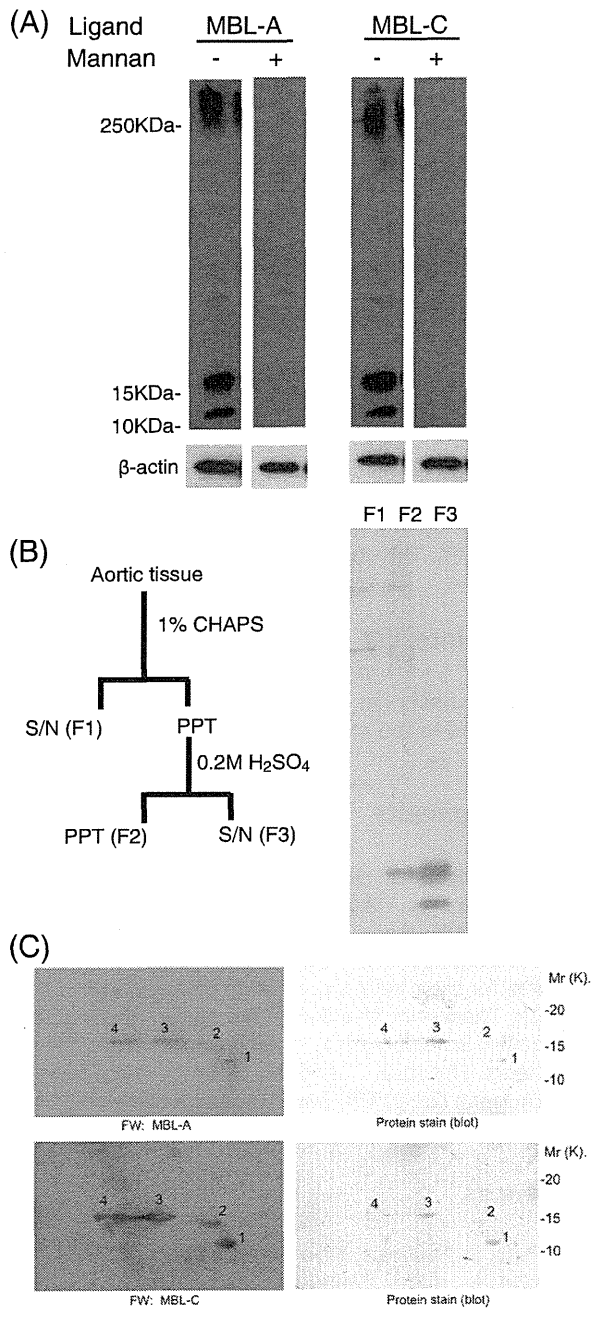

Figure 3 Endogenous targets for mannose-binding lectin (MBL)-A and MBL-C in the aortic tissue. (A) Aortic lysates were subjected to far-western blotting analyses with recombinant murine MBL-A (left side) and MBL-C (right side) and the corresponding antibodies. In some experiments, MBL probing was performed in the presence of yeast mannan as indicated. β-Actin was used as an internal loading control. (B) Aortic proteins were fractionated as shown in the flowchart and then analysed using far-western blotting with MBL-A. MBL-reactive Mr 10–15 kDa proteins were fractionated in Fraction 3. *S/N* and *PPT* stand for 'supernatant' and 'pellet', respectively. (C) Fraction 3 (acid-soluble proteins) was subjected to acid–urea–Triton gel/SDS-gel 2-dimensional gel electrophoresis (AUT/SDS-PAGE), followed by far-western blotting with MBL-A (upper panel) and MBL-C (lower panels). The proteins of interest were identified by liquid chromatography–ion trap mass spectrometry (LC–MS/MS) as follows: Spot 1: Histone H4; Spot 2: Histone H2B -type 1 H; Spot 3: Histone H3.1; Spot 4; Histone H2A-type 2A.

4. Discussion

In the present study, we report that MBL was involved in KD-like murine experimental vasculitis through uncontrolled complement activation. Although the relevance of MBL in KD has been argued on the basis of clinical genetic studies, to the best of our knowledge, the present study is the first to show that humoral innate immune proteins participated in the pathogenesis of vasculitis in a KD animal model.

Further studies are required to address why MBLs preferentially target the aortic root, including the coronary ostium, which is a primary site in CAWS-induced vasculitis. In the present study, we found that MBLs can recognise certain proteins of the aorta and identified histones as one of the major targets for MBLs (Figs. 3C, D and 4). Although histones are primarily nuclear proteins, they are exposed to or released from activated neutrophils or dying cells in the extracellular space [30–32]. Indeed, the marked invasion of activated neutrophils is a hallmark of CAWS-induced KD-like vasculitis [33], suggesting that vasculitis-associated extracellular leakage of these nuclear proteins could result in the recruitment of MBL and MBL-dependent activation of the lectin pathway. In this scenario, MBL may play a pivotal role as an exacerbation factor, rather than as an initiation factor, in vascular inflammation.

The substrates of MBL are considered more diverse than those previously believed. Therefore, along with the histones, MBL may recognise a variety of self-targets, including non-proteinous ones, involved in the pathogenesis

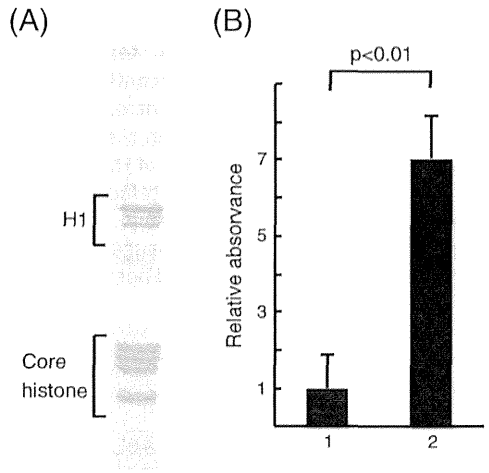

Figure 4 In vitro assay for lectin pathway activation. The lectin pathway activation potential of histones was evaluated in vitro using a Complement System Screen Wieslab kit. Histones were highly purified from DBA2 mouse liver (A). Purified histones were covalently immobilised on a 96-well plate and incubated for 70 min with mannose-binding lectin (MBL)-deficient (B/B) human serum (1) or normal human serum (2) under assay conditions specialised for the lectin pathway. Activation of the lectin pathway was determined by absorbance at 405 nm and represented as a value relative to that obtained from wells of MBL-deficient serum. The data of the assay, which was conducted in triplicate, is shown. Similar results were reproducibly obtained in three independent experiments.

of vasculitis. We don't exclude the possibility that such potential targets are also involved in vasculitis through the activation of the MBL-dependent complement pathway.

The pathophysiological significance of MBL self-reactivity is still controversial and, most likely, situation-dependent. In fact, some studies have reported that MBL is physiologically important for the clearance of dying cells and a first-line defence against a variety of pathogens [34,35]. While the self-reactive innate immune molecules remain below an appropriate level, their adverse effects are thought to be negligible. However, this may not be the case under infectious conditions that are mimicked by CAWS stimulation. When MBLs are markedly upregulated in response to infectious stimuli (Fig. 1), excess MBLs may attack vascular inflammation sites characterised by the invasion of neutrophils to aggravate the vasculitis through the activated lectin pathway.

Little is known about the functional differences between MBL-A and MBL-C. MBL-A gradually increased in the blood in response to CAWS stimulation and MBL-C rapidly disappeared likely because of a change in its distribution from the blood to the spleen (Supplementary data 2) and the aortic root (Fig. 2B). Although further studies are required to address the pathophysiological roles of MBL-C distinct from MBL-A, MBL-C may be involved in splenomegaly, which is observed in the acute phase of the CAWS-administrated murine vasculitis [36,37].

It has been reported that the MBL-dependent lectin pathway co-operates with the IgM-dependent classical pathway to promote tissue damage in some ischemic diseases such as myocardial infarction [28,29]. Considering that the deposition of IgM was detected in the inflamed aortic roots CAWS-induced KD-like vasculitis may underlie the pathogenesis similar to that reported in ischemic diseases. Investigations of this possibility are ongoing in our laboratory.

Considering the physiological roles of MBL, simple suppression of MBL may not necessarily be beneficial in attenuating the vasculitis in KD and CAWS-induced murine vasculitis. Indeed, the potential use of complement pathway inhibitors in ischemia–reperfusion injury is currently argued [38]. However, given that infection-associated vasculitis, such as KD, shares a common pathogenesis with CAWS-induced murine vasculitis, careful pharmacological manipulation of the MBL-dependent complement pathways could be a promising approach for treating KD. Considering that the uncontrolled activation of the complement pathway is associated with the formation of aortic aneurysms [39,40], the MBL-dependent lectin pathway in particular could be a promising therapeutic target for preventing KD-associated coronary artery aneurysms [41].

Supplementary data to this article can be found online at http://dx.doi.org/10.1016/j.clim.2014.03.019.

Authors' contributions

All of the experiments were designed by AN and MO. AN was responsible for the pathological and biochemical experiments presented in this study and wrote the manuscript. CS also contributed to a part of some of the experiments. CAWS was prepared by NM and NO. LC–MS/MS analysis was performed by FK. This study was supervised by KH.

Conflict of interest

None of the authors has any potential financial conflict of interest related to this manuscript.

Acknowledgments

We acknowledge Drs. Maiko Fujii, Tomoyo Yahata, Akiko Hamaoka-Okamoto, Yoko Miwa, Ayako Yoshioka, Seiichiro Ozawa, Kazuyuki Ikeda, Toshiyuki Itoi, Masashi Nishida, Kunitake Fukai, Ryo Ishida, Shinichiro Yamaguchi, and Takesi Shirayama for their help and valuable discussion throughout this work. Thanks are also due to Drs. Kyoko Ito, Sou Tando and Kazuhiro Sonomura for their kind advice on pathological experiments. This study was funded by Grant-in-Aid Scientific Research Japan (23591579) (AN, KH), and a research grant of Japan Kawasaki Disease Research Center (2010) (KH, AN).

References

[1] H. Kato, K. Takahashi, Kawasaki's disease, in: G.V. Ball, S.L. Bridges Jr. (Eds.), Vasculitis, 2nd ed., New York Oxford University Press, 2008, pp. 373–390.

[2] A.B. Hartopo, B.Y. Setianto, Coronary artery sequel of Kawasaki disease in adulthood, a concern for internists and cardiologists, Acta Med Indones. 45 (2013) 69–75.
[3] C.C. Belizna, M.A. Hamidou, H. Levesque, L. Guillevin, Y. Shoenfeld, Infection and vasculitis, Rheumatology (Oxford) 48 (2008) 475–482.
[4] J.M. Yarwood, D.Y. Leung, P.M. Schlievert, Evidence for the involvement of bacterial superantigens in psoriasis, atopic dermatitis, and Kawasaki syndrome, FEMS Microbiol. Lett. 192 (2000) 1–7.
[5] E.J. Sundberg, L. Deng, R.A. Mariuzza, TCR recognition of peptide/MHC class II complexes and superantigens, Semin. Immunol. 19 (2008) 262–271.
[6] P.A. Brogan, V. Shah, L.A. Clarke, M.J. Dillon, N. Klein, T cell activation profiles in Kawasaki syndrome, Clin. Exp. Immunol. 151 (2008) 267–274.
[7] J.D. Fraser, T. Proft, The bacterial superantigen and superantigen-like proteins, Immunol. Rev. 225 (2008) 226–243.
[8] T. Yoshioka, T. Matsutani, S. Iwagami, T. Toyosaki-Maeda, T. Yutsudo, Y. Tsuruta, H. Suzuki, S. Uemura, T. Takeuchi, M. Koike, R. Suzuki, Polyclonal expansion of TCRBV2- and TCRBV6-bearing T cells in patients with Kawasaki disease, Immunology 96 (1999) 465–472.
[9] T. Yoshioka, T. Matsutani, T. Toyosaki-Maeda, H. Suzuki, S. Uemura, R. Suzuki, M. Koike, Y. Hinuma, Relation of streptococcal pyrogenic exotoxin C as a causative superantigen for Kawasaki disease, Pediatr. Res. 53 (2003).
[10] R.S.M. Yeung, The etiology of Kawasaki disease: a superantigen-mediated process, Prog. Pediatr. Cardiol. 19 (2004) 115–122.
[11] T. Uchiyama, H. Kato, The pathogenesis of Kawasaki disease and superantigens, Jpn. J. Infect. Dis. 52 (1999) 141–145 (403-10).
[12] A. Morita, Y. Imada, H. Igarashi, T. Yutsudo, Serologic evidence that streptococcal superantigens are not involved in the pathogenesis of Kawasaki disease, Microbiol. Immunol. 41 (1997) 895–900.
[13] S. Sato, H. Kawashima, Y. Kashiwagi, T. Fujioka, K. Takekuma, A. Hoshika, Association of mannose-binding lectin gene polymorphisms with Kawasaki disease in the Japanese, Int. J. Rheum. Dis. 12 (2009) 307–310.
[14] M.H. Biezeveld, I.M. Kuipers, J. Geissler, J. Lam, J.J. Ottenkamp, C.E. Hack, T.W. Kuijpers, Association of mannose-binding lectin genotype with cardiovascular abnormalities in Kawasaki disease, Lancet 361 (2003) 1268–1270.
[15] M.H. Biezeveld, J. Geissler, G.J. Weverling, I.M. Kuipers, J. Lam, J. Ottenkamp, T.W. Kuijpers, Polymorphisms in the mannose-binding lectin gene as determinants of age-defined risk of coronary artery lesions in Kawasaki disease, Arthritis Rheum. 54 (2006) 369–376.
[16] Y.F. Cheung, M.H. Ho, W.K. Ip, S.F. Fok, T.C. Yung, Y.L. Lau, Modulating effects of mannose binding lectin genotype on arterial stiffness in children after Kawasaki disease, Pediatr. Res. 56 (2004) 591–596.
[17] S. Thiel, M. Gadjeva, Humoral pattern recognition molecules: mannan-binding lectin and ficolins, Adv. Exp. Med. Biol. 653 (2009) 58–73.
[18] M.D. Schafranski, A. Stier, R. Nisihara, I.J. Messias-Reason, Significantly increased levels of mannose-binding lectin (MBL) in rheumatic heart disease: a beneficial role for MBL deficiency, Clin. Exp. Immunol. 138 (2004) 521–525.
[19] R. Malhotra, M.R. Wormald, P.M. Rudd, P.B. Fischer, R.A. Dwek, R.B. Sim, Glycosylation changes of IgG associated with rheumatoid arthritis can activate complement via the mannose-binding protein, Nat. Med. 1 (1995) 237–243.
[20] M.C. Walsh, T. Bourcier, K. Takahashi, L. Shi, M.N. Busche, R.P. Rother, S.D. Solomon, R.A. Ezekowitz, G.L. Stahl, Mannose-binding lectin is a regulator of inflammation that accompanies myocardial ischemia and reperfusion injury, J. Immunol. 175 (2005) 541–546.
[21] H. Ohno, A murine model of vasculitis induced by fungal polysaccharide, Cardiovasc. Hematol. Agents Med. Chem. 6 (2008) 44–52.
[22] K. Takahashi, T. Oharaseki, M. Wakayama, Y. Yokouchi, S. Naoe, H. Murata, Histopathological features of murine systemic vasculitis caused by *Candida albicans* extract—an animal model of Kawasaki disease, Inflamm. Res. 53 (2004) 72–77.
[23] N. Nagi-Miura, T. Harada, H. Shinohara, K. Kurihara, Y. Adachi, A. Ishida-Okawara, T. Oharaseki, K. Takahashi, S. Naoe, K. Suzuki, N. Ohno, Lethal and severe coronary arteritis in DBA/2 mice induced by fungal pathogen, CAWS, *Candida albicans* water-soluble fraction, Atherosclerosis 186 (2006) 310–320.
[24] W.M. Bonner, M.H. West, J.D. Stedman, Two-dimensional gel analysis of histones in acid extracts of nuclei, cells, and tissues, Eur. J. Biochem. 109 (1980) 17–23.
[25] F. Kametani, T. Nonaka, T. Suzuki, T. Arai, N. Dohmae, H. Akiyama, M. Hasegawa, Identification of casein kinase-1 phosphorylation sites on TDP-43, Biochem. Biophys. Res. Commun. 382 (2009) 405–409.
[26] K. Kurihara, Y. Shingo, N. Miura, S. Horie, Y. Usui, Y. Adachi, T. Yadomae, N. Ohno, Effect of CAWS, a mannoprotein-beta-glucan complex of *Candida albicans*, on leukocyte, endothelial cell, and platelet functions in vitro, Biol. Pharm. Bull. 26 (2003) 233–240.
[27] K.J. Shields, D. Stolz, S.C. Watkins, J.M. Ahearn, Complement proteins C3 and C4 bind to collagen and elastin in the vascular wall: a potential role in vascular stiffness and atherosclerosis, Clin. Transl. Sci. 4 (2011) 146–152.
[28] R.K. Chan, S.I. Ibrahim, K. Takahashi, E. Kwon, M. McCormack, A. Ezekowitz, M.C. Carroll, F.D. Moore Jr., W.G. Austen Jr., The differing roles of the classical and mannose-binding lectin complement pathways in the events following skeletal muscle ischemia–reperfusion, J. Immunol. 177 (2006) 8080–8085.
[29] M.N. Busche, V. Pavlov, K. Takahashi, G.L. Stahl, Myocardial ischemia and reperfusion injury is dependent on both IgM and mannose-binding lectin, Am. J. Physiol. Heart Circ. Physiol. 297 (2009) H1853–H1859.
[30] K. Kessenbrock, M. Krumbholz, U. Schönermarck, W. Back, W.L. Gross, Z. Werb, H.J. Gröne, V. Brinkmann, D.E. Jenne, Netting neutrophils in autoimmune small-vessel vasculitis, Nat. Med. 15 (2009) 623–625.
[31] E. Villanueva, S. Yalavarthi, C.C. Berthier, J.B. Hodgin, R. Khandpur, A.M. Lin, C.J. Rubin, W. Zhao, S.H. Olsen, M. Klinker, D. Shealy, M.F. Denny, J. Plumas, L. Chaperot, M. Kretzler, A.T. Bruce, M.J. Kaplan, Netting neutrophils induce endothelial damage, infiltrate tissues, and expose immunostimulatory molecules in systemic lupus erythematosus, J. Immunol. 187 (2011) 538–552.
[32] M. Radic, T. Marion, M. Monestier, Nucleosomes are exposed at the cell surface in apoptosis, J. Immunol. 172 (2004) 6692–6700.
[33] A. Ishida-Okawara, N. Nagi-Miura, T. Oharaseki, K. Takahashi, A. Okumura, H. Tachikawa, S. Kashiwamura, H. Okamura, N. Ohno, H. Okada, P.A. Ward, K. Suzuki, Neutrophil activation and arteritis induced by *C. albicans* water-soluble mannoprotein-beta-glucan complex (CAWS), Exp. Mol. Pathol. 82 (2007) 220–226.
[34] K. Takahashi, Mannose-binding lectin and the balance between immune protection and complication, Expert Rev. Anti-Infect. Ther. 9 (2001) 1179–1190.
[35] L.M. Stuart, K. Takahashi, L. Shi, J. Savill, R.A. Ezekowitz, Mannose-binding lectin-deficient mice display defective apoptotic cell clearance but no autoimmune phenotype, J. Immunol. 174 (2005) 3220–3226.
[36] T.S. Ingrid, J. Whitbred, B. Dahms, K. Suzuki, N. Miura, N. Ohno, R. Whitbred, Importance of Fcg RI&III and CD11b in susceptibility and immune response to CAWS induced coronary angiitis/aortitis, Arthritis Rheum. 60 (Suppl. 10) (2009) 322.

[37] G. Ohshio, F. Furukawa, H. Fujiwara, Y. Hamashima, Hepatomegaly and splenomegaly in Kawasaki disease, Pediatr. Pathol. 4 (1985) 257–264.
[38] M. Osthoff, G. Trendelenburg, D.P. Eisen, M. Trendelenburg, Mannose-binding lectin—the forgotten molecule? Nat. Med. 17 (2011) 1547–1548.
[39] I. Hinterseher, R. Erdman, L.A. Donoso, T.R. Vrabec, C.M. Schworer, J.H. Lillvis, A.M. Boddy, K. Derr, A. Golden, W.D. Bowen, Z. Gatalica, N. Tapinos, J.R. Elmore, D.P. Franklin, J.L. Gray, R.P. Garvin, G.S. Gerhard, D.J. Carey, G. Tromp, H. Kuivaniemi, Role of complement cascade in abdominal aortic aneurysms, Arterioscler. Thromb. Vasc. Biol. 31 (2011) 1653–1660.
[40] M.B. Pagano, H.F. Zhou, T.L. Ennis, X. Wu, J.D. Lambris, J.P. Atkinson, R.W. Thompson, D.E. Hourcade, C.T. Pham, Complement-dependent neutrophil recruitment is critical for the development of elastase-induced abdominal aortic aneurysm, Circulation 119 (2009) 1805–1813.
[41] L.B. Daniels, J.B. Gordon, J.C. Burns, Kawasaki disease: late cardiovascular sequelae, Curr. Opin. Cardiol. 27 (2012) 572–577.

Hamaoka-Okamoto *et al. Pediatric Rheumatology* 2014, **12**:12
http://www.ped-rheum.com/content/12/1/12

PEDIATRIC
RHEUMATOLOGY

RESEARCH Open Access

The involvement of the vasa vasorum in the development of vasculitis in animal model of Kawasaki disease

Akiko Hamaoka-Okamoto[1*], Chinatsu Suzuki[1], Tomoyo Yahata[1], Kazuyuki Ikeda[1], Noriko Nagi-Miura[2], Naohito Ohno[2], Yoshinori Arai[3], Hideo Tanaka[4], Tetsuro Takamatsu[4] and Kenji Hamaoka[1]

Abstract

Background: Kawasaki Disease (KD) involves a diffuse and systemic vasculitis of unknown etiology that mainly affects infants and children. Although a considerable number of analyses of the clinical, histopathological and molecular biological details underlying the mechanism responsible for the development of coronary arterial lesions, it is still poorly understood.
The purpose of this study was to analyze the state of angiogenesis, vasculogenesis and the distribution of blood vessels using an animal model of KD like vasculitis. We investigated the involvement of the vasa vasorum from the adventitia in the vascular involvement and the development of the disease state by performing sequential histopathology, scanning electron microscopy (SEM) and micro computed tomography (CT) studies using a murine model of vasculitis induced by the *Candida albicans* water-soluble fraction (CAWS).

Methods: To prepare the animal model of KD like vasculitis, CAWS was intraperitoneally injected into C57BL/6N mice for five consecutive days as reported by *Ohno et al.* We observed the changes of the vasa vasorum at the aorta and the orifices of the coronary arteries by SEM and micro CT, and also compared the neovascularization at the media and adventitia of the aorta by an immunohistochemical analysis.

Results: As previously reported, obvious inflammation was detected two weeks after the injection of CAWS, and also intimal thickening was observed three weeks after the injection. We found that the vasa vasorum in the adventitia of the aorta was increased in the model mice. The vasa vasorum started increasing one week after the injection of CAWS, before any obvious vasculitis was microscopically detected.

Conclusion: The present results indicate that the vasculitis in Kawasaki disease starts as a disorder of the vasa vasorum.

Keywords: Kawasaki disease, A murine model, Vasculitis, Adventitia, Vasa vasorum

Background

Kawasaki disease (KD) involves diffuse, systemic vasculitis of unknown etiology and pathogenesis, and predominantly affects infants and children [1-3]. The incidence of KD has steadily increased since it was first reported, and more than 12,000 people are diagnosed with KD each year in Japan. The well-known sequelae of KD include coronary aneurysms, which occur in approximately 5% of the KD patients [4]. With time, an aneurysm may cause stenotic lesions or ischemic heart disease, even in children [5-7].

Intravascular immunoglobulin (IVIG) therapy can greatly decrease the chances of complications of coronary arterial lesions (CALs), though 10–15% of the patients are refractory to IVIG. In these cases, the incidence of CALs tends to be much higher.

Since KD was first described by Kawasaki in 1967, many clinical, histopathological and or molecular biological studies have been performed to investigate the

* Correspondence: ahamaoka@koto.kpu-m.ac.jp
[1]Department of Pediatric Cardiology and Nephrology, Kyoto Prefectural, University of Medicine Graduate School of Medical Science, Kamigyo-ku, Kyoto 602-8566, Japan
Full list of author information is available at the end of the article

pathophysiology of the vascular involvement of KD; however, the underlying mechanism remains unclear [2,3,8,9]. Coronary arteritis in KD is considered to begin with edematous changes in the media, developing into inflammatory changes in the intima and adventitia, which finally evolve into the panvasculitis observed during autopsies [8].

In contrast, recent studies using various animal models of KD like vasculitis have indicated that the inflammatory changes in the adventitia occur prior to the changes in the intima [10-12]. In 1975, Onouchi et al. suggested that the vasa vasorum, which supplies nutrition to the walls of blood vessels, might contribute to the progression of vasculitis in KD, beginning with severe tissue destruction at the vasa vasorum in the adventitia [9]. Although there have not been detailed pathological studies on the significance of the vasa vasorum in KD, recent studies using the advanced imaging analyses have shown that the abnormal proliferation of the vasa vasorum was associated with plaque formation and the destabilization of lesions during the development of arterial sclerosis. In chronic inflammatory diseases such as arterial sclerosis, the abnormal proliferation of the vasa vasorum may provide an infiltrative route for inflammatory cells from the adventitia, and this accumulation of inflammatory cells promotes the inflammation [13-15]. Thus, we hypothesized that the vasa vasorum might serve as the initiator of vasculitis in KD.

Various animal models have been developed to investigate KD vasculitis. In 1979, Murata and Naoe et al. first reported that the *Candida albicans* derived substance (CADS) isolated from the feces of patients with KD causes coronary arteritis as seen in KD [16]. Subsequent studies revealed that the water-soluble extracellular polysaccharide fraction (CAWS) obtained from the culture supernatant of *Candida albicans* resulted in a stronger but similar vasculitis that occurred more frequently than that following exposure to CADS. Therefore, CAWS-induced vasculitis has become widely adopted as a universal animal model for KD like vasculitis [17-25].

The purpose of this study was to delineate the involvement of the vasa vasorum in the development of KD vasculitis by examining its proliferation and distribution using histopathological or micro-computed tomography (CT) and scanning electron microscope (SEM) studies. KD is associated with a low mortality rate, and due to the low availability of autopsied hearts, we used the CAWS animal model for this purpose.

Methods

Animals

All experimental procedures were approved by the Committee for Animal Research, Kyoto Prefectural University of Medicine. A total of 24 four-week-old male C57BL/6N mice were obtained from SHIMIZU Laboratory Supplies Co., Ltd. (Kyoto, Japan) and were randomly divided into six experimental groups: control and model mice evaluated at one week, two weeks and three weeks after the administration of CAWS.

CAWS was kind gift from Tokyo University of Pharmacy and Life Science and 0.2 mL (20 mg/mL) was administered intraperitoneally to the model mice daily for five consecutive days starting at the age of five weeks.

Histopathology

After heparin was administered, anesthesia was induced with a fatal dose of pentobarbital sodium. The chest was then opened, and the abdominal aorta was cannulated and infused with saline until the venous effluent was free of blood. Sections of the heart at the level of the aortic valves were obtained.

Tissue specimens were fixed in 20% formalin, embedded in paraffin and sectioned at 4 μm-thick slices. First, hematoxylin and eosin (HE)- and elastic van Gieson (EVG)-stained sections were examined by light microscopy.

Next, immunohistochemical studies for CD3 and MPO were performed to detect the type of inflammatory cells. Some sections were deparaffinized in xylene and ethanol rinses. Only sections for CD3 were activated by boiling for 5 min in a citrate buffer (0.01 M) at pH 9.0 in a microwave. No pretreatment was needed for MPO. After blocking of non- specific binding, the sections were incubated at 4 °C overnight in a humidified slide chamber with polyclonal antibodies (Dako Cytomation) for CD3 (dilution 1:400) and MPO (dilution 1:600). After incubation with the corresponding secondary antibody for 30 minutes, the antibody binding was revealed using H_2O_2 and diaminobenzidine. Counterstaining was performed with hematoxylin, and sections were examined by light microscopy.

Immunofluorescent studies were also performed using Biotin-conjugated Isolectin IB_4 (Molecular Probes, Inc.). Some sections were deparaffinized in xylene and ethanol rinses, and activated by boiling for 5 min in a citrate buffer (0.01 M) at pH 6.0 in a microwave. The sections were incubated at 4°C overnight in a humidified slide chamber with lectin diluted at 1:200. The stained specimens were observed using a confocal laser scanning microscope (LSM510 ver. 4.0; Carl Zeiss CO., Ltd., Oberkochen, Germany).

SEM

To examine the types of vessels, we investigated the adventitia of the micro- vessels using SEM [26]. After administering lethal anesthesia with pentobarbital sodium, a blue synthetic resin (Mercox®, DIC, Tokyo) was injected through a 22 Ga plastic needle inserted into the left ventricle. The sample was maintained at room

temperature until the liquid resin was completely polymerized. The heart, aorta and perivascular soft tissues were then harvested *en bloc*. The soft tissues were dissolved by incubation in 20% potassium hydroxide solution at 50°C for three days. To completely dissolve the fat tissues, the samples were incubated with proteinase K in buffer ATL for one day. Then, the samples were washed in 0.5% Nonidet P-40. The microvascular casts were mounted on stubs, coated with osmium and examined using SEM (JSM-6320 F; JEOL, Tokyo).

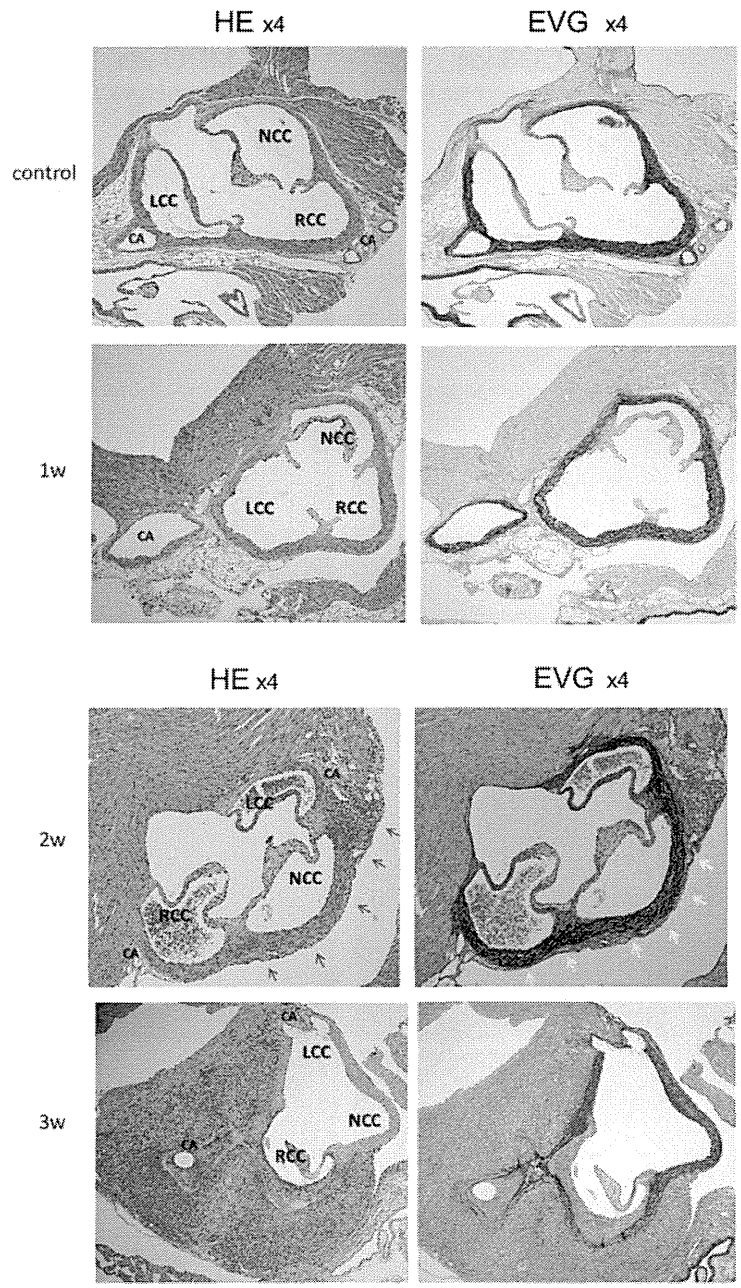

Figure 1 The four developmental stages in the murine model of Kawasaki disease like vasculitis based on the histopathological analysis. In hematoxylin and eosin (HE)-stained sections, there were some inflammatory cells visible in the adventitia one week after the CAWS injection (red arrows). Obvious infiltration of inflammatory cells was detected more than two weeks after the injections of the *Candida albicans* water-soluble fraction (CAWS) (red arrows). Three weeks after the injection, marked adventitial thickening was detected.In elastica van Gieson (EVG)-stained sections, the elastic fibers started to be destroyed more than two weeks after the injections of CAWS (yellow arrows). RCC: Right Coronary Cusp, LCC: Left Coronary Cusp, NCC: Non Coronary Cusp, CA: Coronary Artery.

Micro CT

After lethal anesthesia with pentobarbital sodium was induced, the thorax was opened. The abdominal aorta was cannulated and infused with heparinized saline until the venous effluent was free of blood. Next, the OMNIPAQUE 240 contrast agent was infiltrated from the abdominal aorta at a steady rate.

The aorta and coronary arteries were scanned *en bloc* by a micro CT system (Rigaku, Tokyo, Japan) [27-29]. The resulting three-dimensional images were displayed using the i-view software program (Morita, Kyoto, Japan). The number of pixels used to reconstruct the images was 500 × 500 × 500, and the time required for filming and reconstruction was

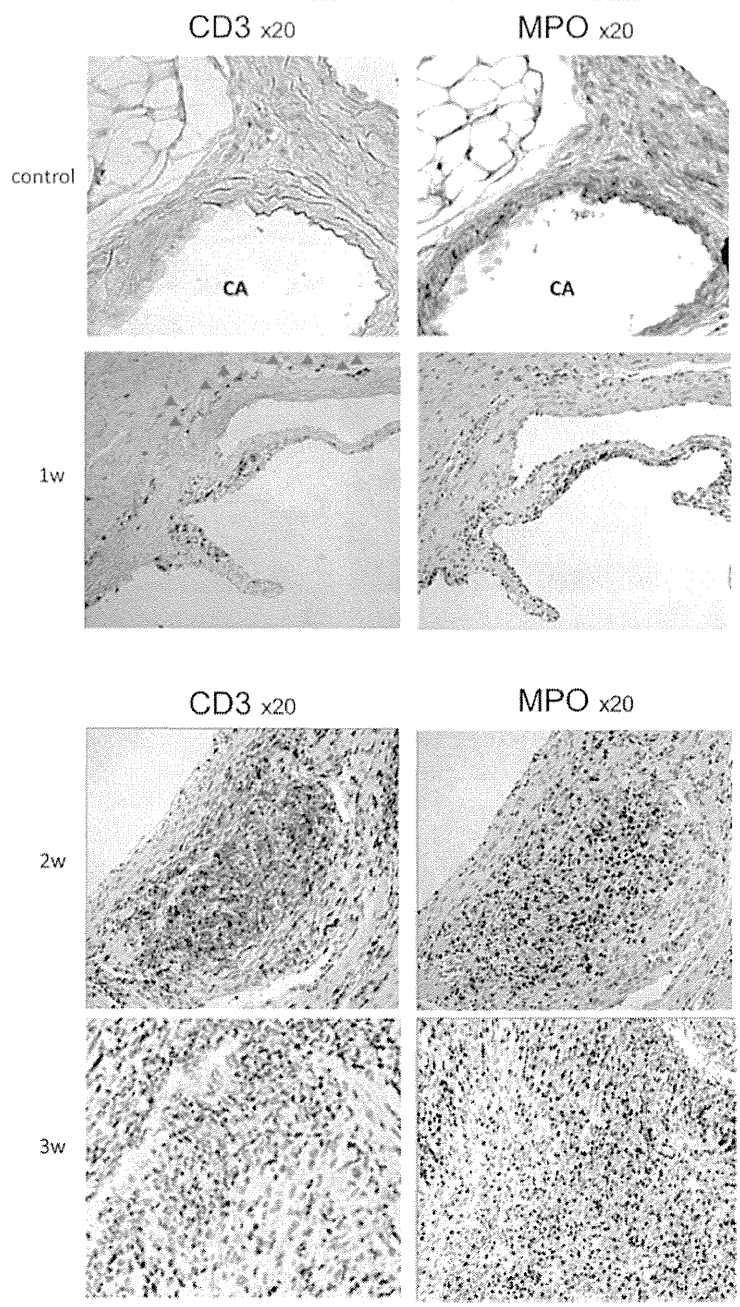

Figure 2 The results of the sections stained with antibodies for CD3 and MPO. In only sections with antibody for CD3, there were some CD3 positive cells visible at the same position inflammatory cells were detected one week after the *Candida albicans* water-soluble fraction (CAWS) injection (red triangles). More CD3 positive cells and some MPO positive cells were detected around coronary arteries more than two weeks after the injections of the injection. Three weeks after the injection, more MPO positive cells were detected.

two minutes. It was also possible to examine a three-dimensional tomographic image simultaneously. The pixel size was 10 μm, and the filming span was 5 mm × 5 mm.

Results

Histopathology

One week after the CAWS injection, there were some inflammatory cells visible in the adventitia. Two weeks after the injection, there was clear infiltration of inflammatory cells and destruction of the elastic fibers. Marked adventitial thickening was detected at time points three or more weeks after the injection (Figure 1) [25].

Next, immunohistochemical studies were performed to observe the type of inflammatory cells using antibodies for CD3 and MPO. One week after the CAS injection, there were some CD3 positive cells only around aorta, at the same position inflammatory cells were detected by HE stain. Two weeks after the injection, more CD3 positive cells and some MPO positive cells were detected even around coronary arteries. More MPO positive cells were observed at time points three or more weeks after the injection (Figure 2). These results by HE stain and immunostain revealed the inflammatory cells consisted on monocytes, lymphocytes and neutrophils.

Immunofluorescent studies were also performed to observe the appearance of the inflammatory cells at the adventitia and their infiltration inward, and we found small vessels that were not detected in control mice. Figure 3 shows the sections stained with Isolectin. Compared with the controls, some lectin- positive endothelial cells were visible only at the adventitia of the aorta one week after the injection of CAWS. Similar to the inflammatory cells, the lectin-positive cells had infiltrated inward two weeks after the injection, and by the following week, these cells filled all layers.

It has been demonstrated that the vasa vasorum provides a considerable amount of blood flow to the adventitia and one- third of the outer layer of the media [30-32]. Therefore, the blood vessels in the adventitia are part of the vasa vasorum or its branches.

We also examined the size and distribution of the vasa vasorum. As shown in Figure 4, the vasa vasorum proliferated as the inflammation developed.

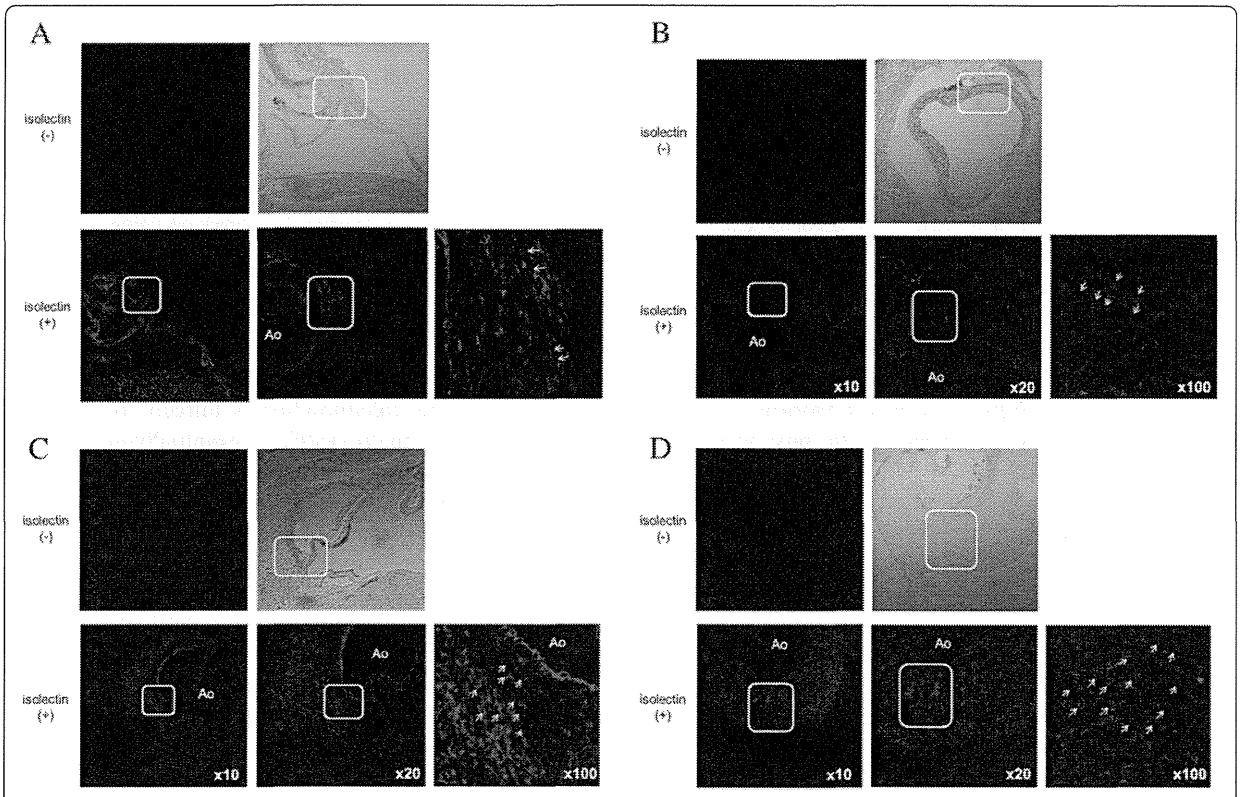

Figure 3 The results of the sections stained with Isolectin. A: A representative control mouse. Only a few Isolectin-positive endothelial cells were detected at the adventitia. **B**: A model mouse one week after the injection of *Candida albicans* water-soluble fraction (CAWS). Compared to the control, there were more Isolectin-positive endothelial cells detected at the adventitia. **C**: A model mouse two weeks after the injection of CAWS. The Isolectin-positive cells had infiltrated inward. **D**: A model mouse three weeks after the injection of CAWS. The Isolectin-positive cells infiltrated all layers.